SUPPLEMENTARY INFORMATION

Two-fold proton coupled electron transfer of a Ta(V) aniline complex mediated by a redox active NNN pincer ligand

Sotirios Pavlidis,[a] Jasmin Alasadi,[a] Amanda Opis-Basilio[a] and Josh Abbenseth*[a]

a Institut für Chemie, Humboldt-Universität zu Berlin, Brook-Taylor-Str. 2, 12489 Berlin, Germany. E-Mail: josh.abbenseth@hu.berlin.de

Table of content

Synthetic Procedures

Ligand Synthesis

The synthesis of compounds **A** – **^{H3}NNN^{cat}** follows a published procedure with several modifications on a larger scale.[1-4]

Multi-step synthesis of 2,7,9,9-tetramethyl-9,10-dihydro-acridine (A)

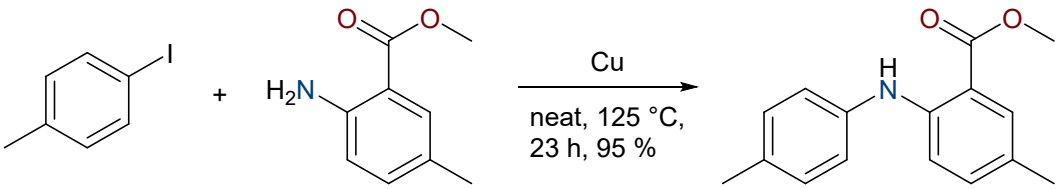

Methyl 2-amino-5-methyl benzoate (12.0 g, 72.6 mmol, 1.0 eq.), 4-Iodotoluene (15.8 g, 72.6 mmol, 1.0 eq.), K_2CO_3 (10.0 g, 72.6 mmol, 1.0 eq.) and copper powder (690 mg, 10.9 mmol, 15 mol%) are added into a pressure tube and set under argon atmosphere. The reaction mixture is stirred at 125 °C for 23 h. The bright brown reaction suspension is cooled to 25 °C and diluted with an $CHCl_3$ / H_2O mixture followed by extraction with $CHCl_3$ (4 x 50 mL), washed with brine (4 x 50 mL), the combined organic phases are dried over $MgSO_4$. Filtration and removing the solvent under reduced pressure leads to a yellow oil (17.6 g, 68.8 mmol, 95%)
^{1}H NMR spectra matched published spectra.[5]

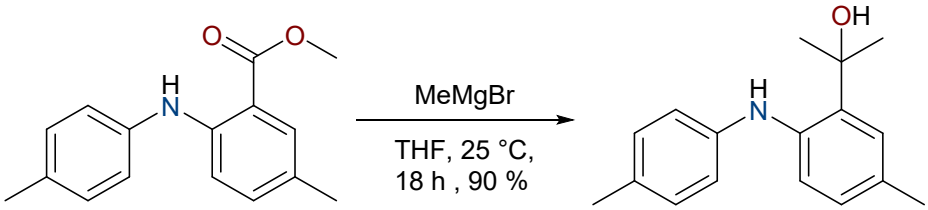

The above obtained oil (17.6 g, 68.8 mmol, 1.0 eq.) is set under argon atmosphere, dissolved in dry THF (200 mL) and cooled to 0 °C. While stirring the amber coloured solution, MeMgBr (100 mL, 3 M in Et_2O, 4.4 eq.) is added dropwise. The bright orange reaction mixture is slowly warmed to 25 °C and stirred for 18 h. To quench residual Mg organyls as well as hydrolyse the compound, the reaction mixture is cooled to 0 °C and quenched with water (5.40 mL) then with HCl (300 mL, 2 M). The resulting bright orange solution is extracted with Et_2O (4 x 30 mL), washed with brine (4 x 50 mL) and the combined organic phases are dried over $MgSO_4$, filtration and removing the solvent under reduced pressure leads to a yellow / brown oil (15.8 g, 61.9 mmol, 90%)
^{1}H NMR spectra matched published spectra.[5]

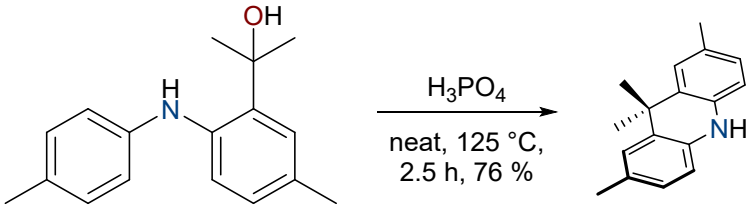

A

The above obtained oil (15.8 g, 61.9 mmol, 1.0 eq.) is suspended in H_3PO_4 (85 %, 60 mL) and heated to 125 °C for 2.5 h. Afterwards the reaction solution is cooled to 0 °C and diluted with water and Et_2O followed by extraction with Et_2O (4 x 30 mL). The aqueous phase and organic phases are collected separately. The aqueous phase is neutralized with NaOH (580 mL, 3 M) until a pH of 7-8 is reached and further extracted with Et_2O (4 x 30 mL). The combined organic phases are washed with water (100 mL) and brine (3 x 50 mL), dried over $MgSO_4$ and the solvent is removed under reduced pressure. 9,10-Dihydro-2,7,9,9-tetramethylacridine (**A**) is obtained as a red waxy solid (13.1 g, 55.0 mmol, 76%)
^{1}H NMR spectra matched published spectra.[5]

Synthesis of B

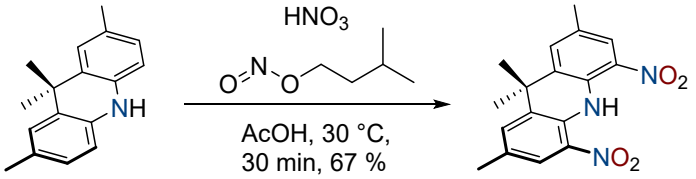

A **B**

A (2.00 g, 8.43 mmol, 1.0 eq.) is dissolved in AcOH (150 mL). While stirring, HNO_3 (68%, 4 mL) is added quickly followed by a dropwise addition of isopentyl nitrite (3.4 mL, 25.3 mmol, 3.0 eq.). The bright red suspension is stirred for 30 min at 25 °C followed by filtration over a Büchner funnel and washing with water (400 mL). **B** is obtained as a partially crystalline red powder (1.86 g, 5.68 mmol, 67%).
^{1}H NMR spectra matched published spectra.[3]

Synthesis of C

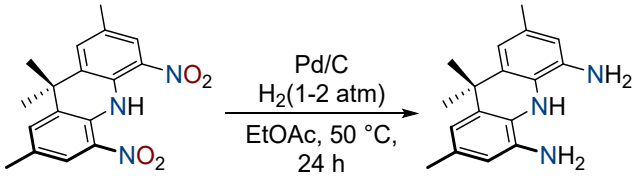

B **C**

B (1.05 g, 3.21 mmol, 1.00 eq.) and Pd/C (10 w%, 0.154 mmol, 5 mol%) are suspended in EtOAc (40 mL) under aerobic conditions. The reaction suspension is degassed with three freeze-pump-thaw cycles, backfilled with H_2 (2 atm, exc.) and stirred for 24 h at 50 °C. The slightly yellow solution is filtered into a new Schlenk flask and the solvent is removed under reduced pressure. **C** is obtained as a light-yellow solid (823.5 mg, 3.08 mmol, 96%)
^{1}H NMR spectra matched published spectra.[3]

Synthesis of D

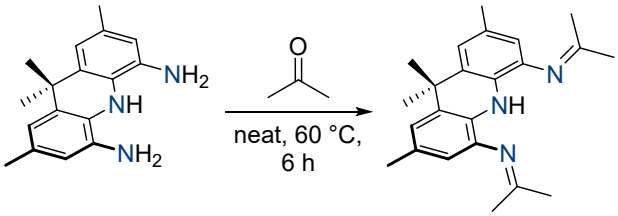

C **D**

C (825 mg, 3.09 mmol, 1.0 eq.) and $MgSO_4$ (1.03 g, 8.59 mmol, 2.8 eq.) are suspended in freshly distilled and degassed acetone (25 mL) under inert conditions. The slightly yellow reaction suspension is heated to 60 °C and refluxed for 6 h. After cooling the reaction solution to 25 °C the solution is filtered into a new flask and the solvent is removed under reduced pressure. **D** is obtained as a yellow waxy solid that is directly used for the synthesis of **^{H3}NNN^{cat}**.

NMR: (C_6D_6, 25 °C): ^{1}H (400 MHz) δ (ppm): 7.08 – 7.03 (m, 2H, $C_{3/11}CH$), 6.97 (s, 1H, N*H*), 6.37 (dd, *J* = 1.9, 0.8 Hz, 2H, $C_{5/9}H$), 2.28 (s, 6H, $C_{20/23}H_3$), 2.00 (s, 6H, $C_{15/18}CH_3$), 1.67 (s, 6H, $C_{21/22}H_3$), 1.50 (s, 6H, $C_{16/19}CH_3$).
NMR: (C_6D_6, 25 °C): ^{13}C{1H} (75 MHz) δ (ppm) = 170.35 ($C_{14/17}$), 136.38 ($C_{1/13}$), 129.70 (C_4), 129.16 (C_7), 128.50($C_{2/12}$), 121.34 ($C_{3/11}$), 117.82 ($C_{5/9}$), 37.12 ($C_{6/8}$), 30.45 ($C_{21/22}$), 28.47 ($C_{15/18}$), 21.47 ($C_{20/23}$), 20.31 ($C_{16/19}$).

Synthesis of ^{H3}NNN^{cat}

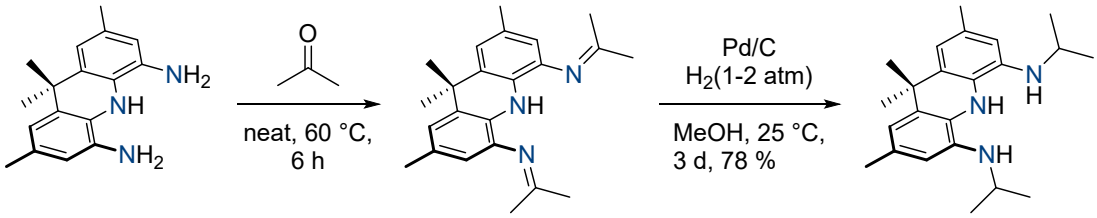

C **D** **^{H3}NNN^{cat}**

To **C** (825 mg, 3.09 mmol, 1.0 eq.) Pd/C (10 w%, 0.305 mmol, 10 mol%) is added in an argon counter flow. The substrates are suspended in dry MeOH (20 mL) and acetone (100 µl, 13.5 mmol,4.4 eq.) is added. The reaction mixture is degassed, backfilled with H_2 and stirred for 3 d at 30 °C. Filtration of the colourless solution into a new flask and removing solvent under reduced pressure gives an off-white powder (842.8 mg, 2.40 mmol, 78%).
^{1}H NMR spectra matched published spectra.[9]

Spectroscopic data (Ligand synthesis)

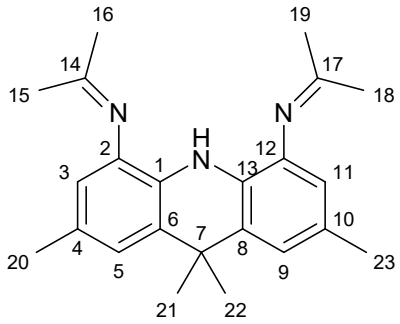

Scheme S1. Carbon numbering of the NNN Ligand for NMR signal assignment.

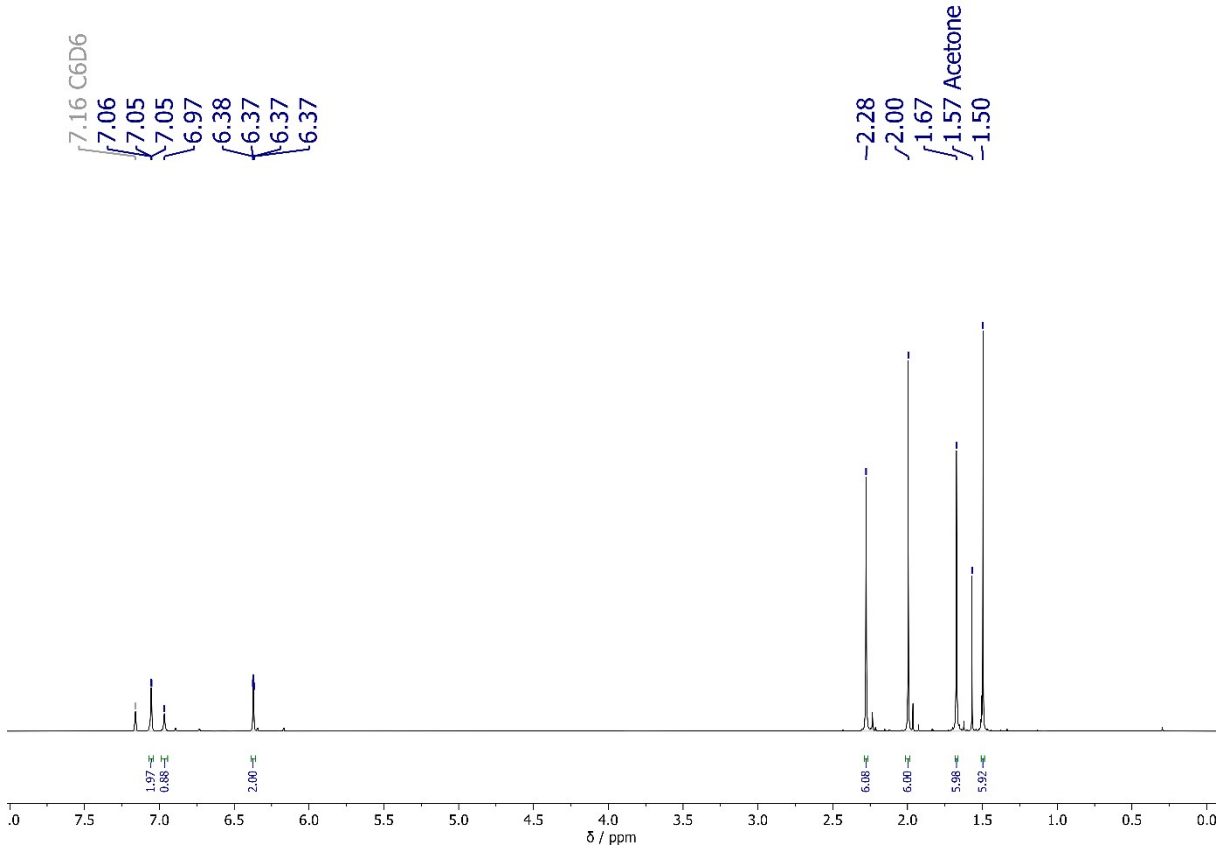

Figure S1. ^{1}H NMR spectrum of **D**, C_6D_6, 25 °C.

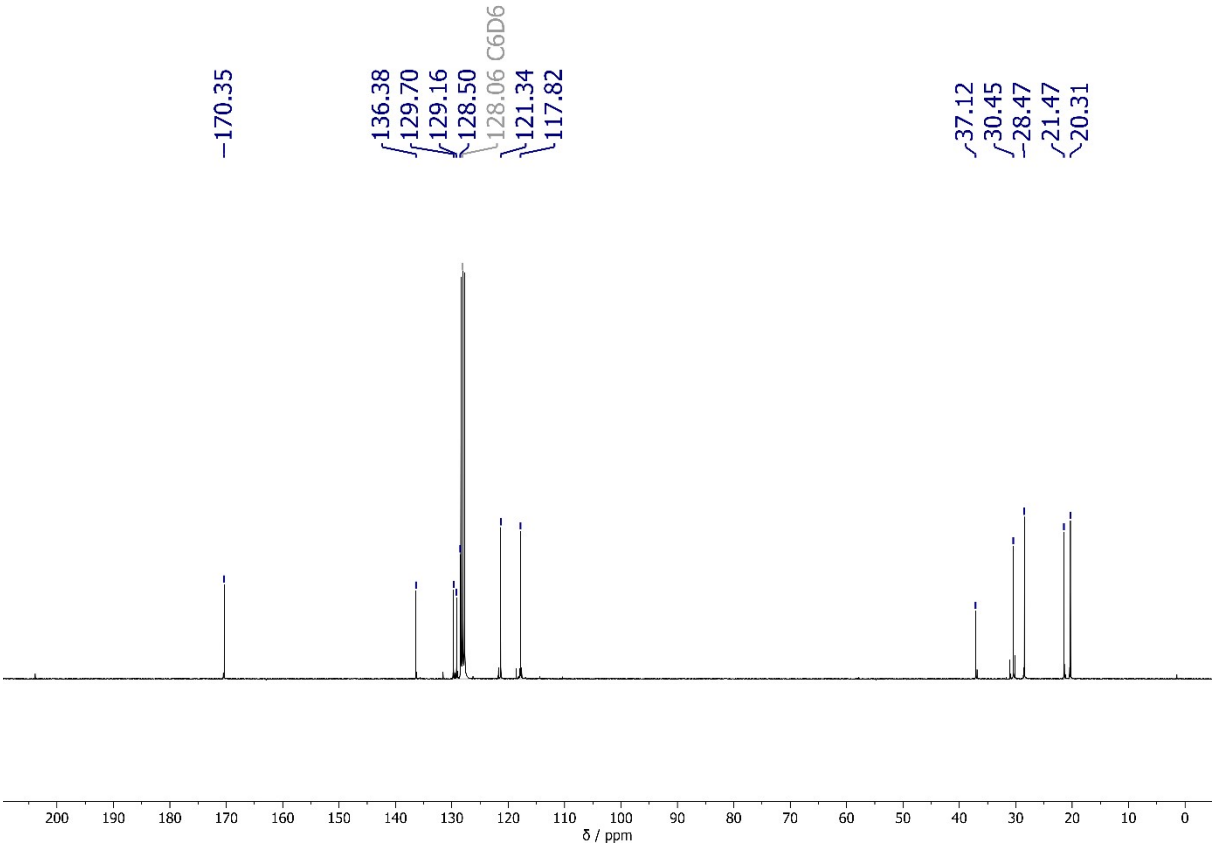

Figure S2. $^{13}C\{^{1}H\}$ NMR spectrum of **D**, C_6D_6, 25 °C.

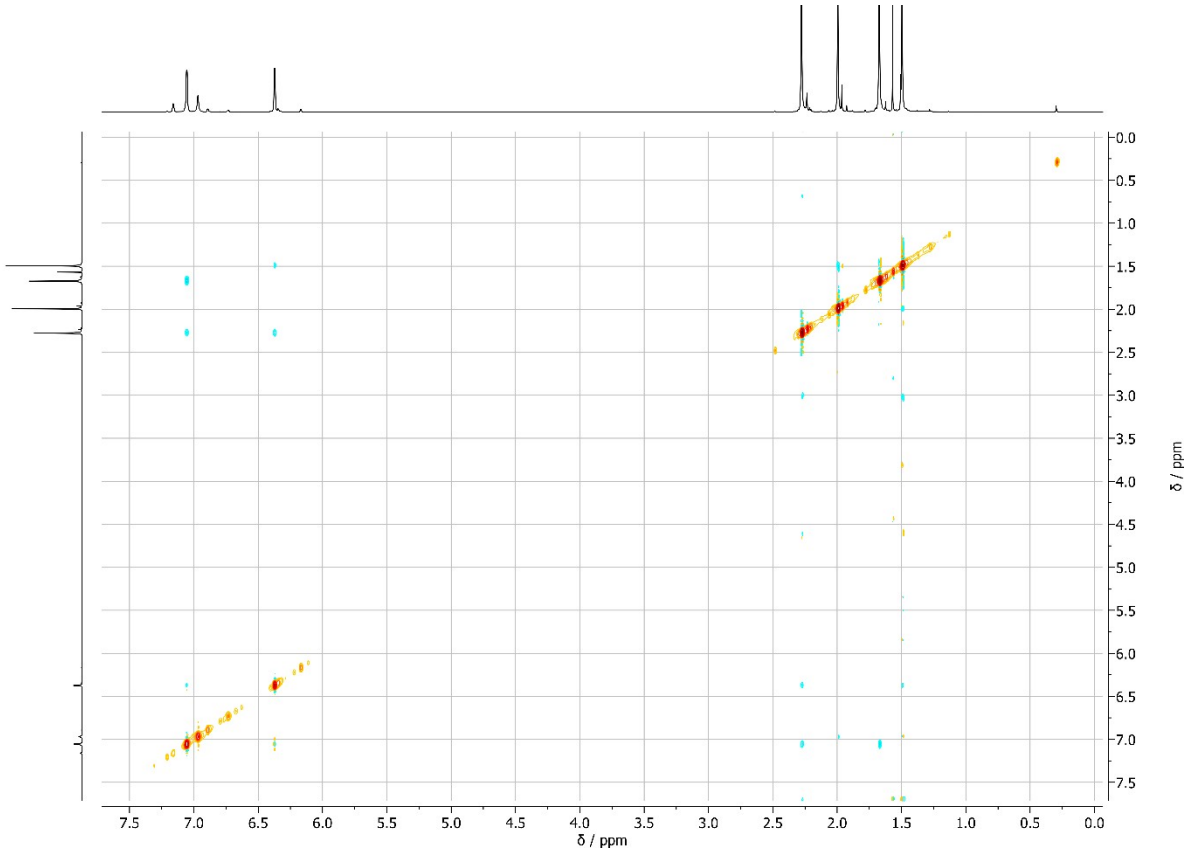

Figure S3. HSQC spectrum of **D**, C_6D_6, 25 °C.

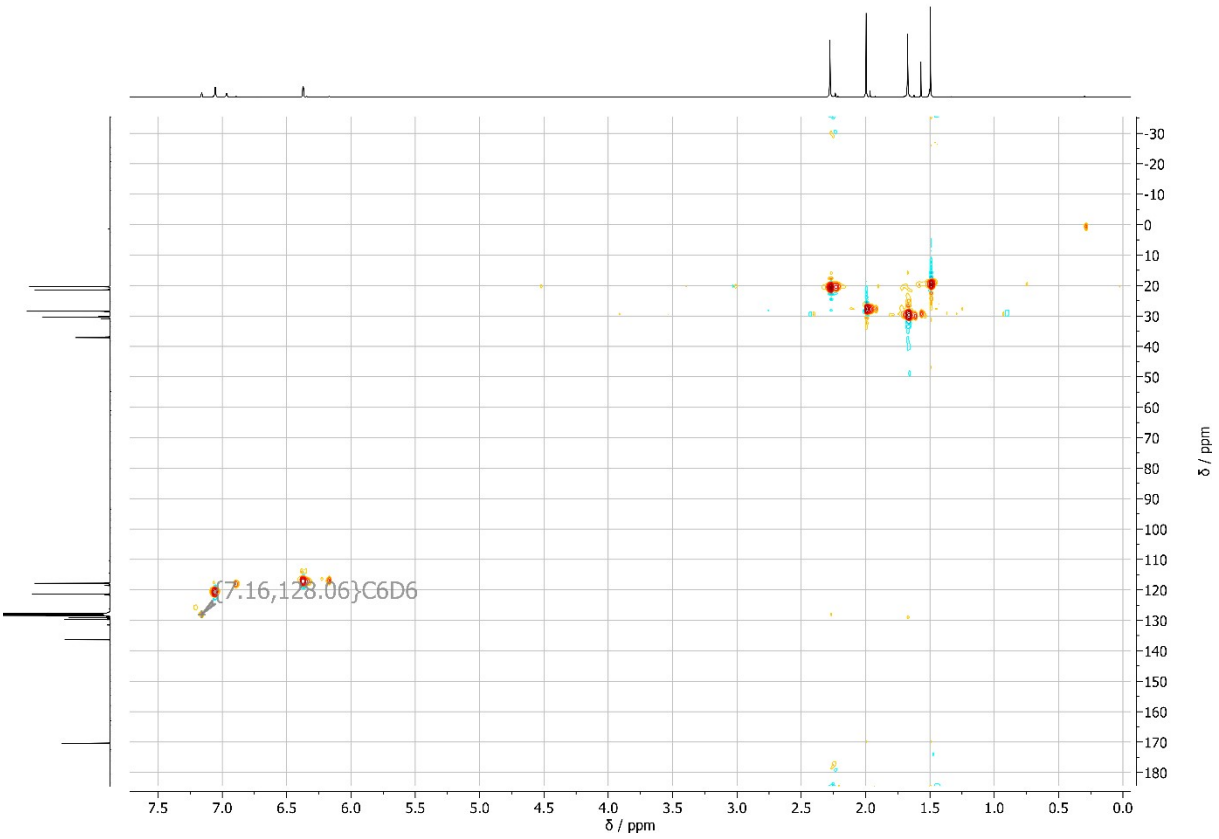

Figure S4. HMBC spectrum of **D**, C_6D_6, 25 °C.

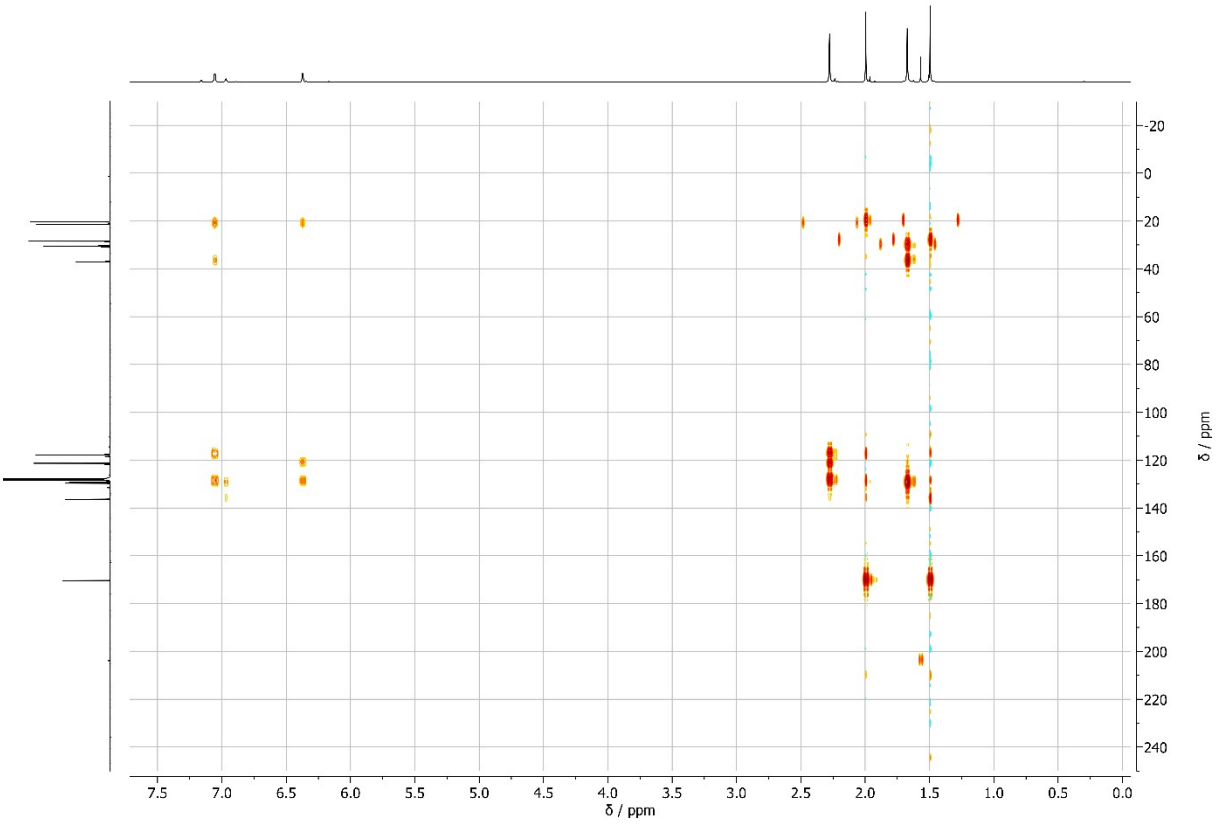

Figure S5. NOESY spectrum of **D**, C_6D_6, 25 °C.

Further reactions of Ta coordination compounds

3 + TEMPOH

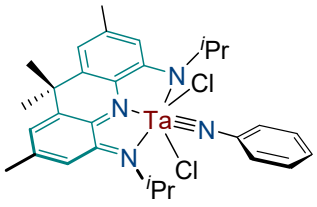

3

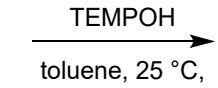

(no reaction)

To a solution of **3** (10 mg, 14.5 µmol, 1.0 eq.) toluene-d_8 TEMPOH (4.6 mg, 28.9 µmol, 2.0 eq.) is added and examined via NMR-spectroscopy.

I + diazobenzene

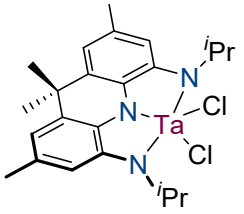

I

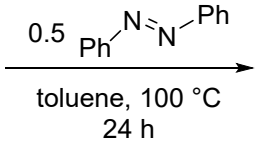

(no reaction)

^{H3}**NNN**^{cat} (10.0 mg, 28.5 µmol, 1.0 eq.) is dissolved in toluene-d_8 (0.3 mL) and added to a solution of $TaMe_3Cl_2$ (8.5 mg, 28.45 µmol, 1.0 eq.) in toluene (0.2 mL). Heating the reaction solution to 100 °C for 1 h results in gas evolution and a bright red colour. Azobenzene (2.6 mg, 14.3 µmol, 0.5 eq.) is added to the reaction mixture, after 30 min at 34 °C no colour change was observed. The reaction mixture is heated for 24 h at 100 °C. No conversion of the substrate could be observed in the ^{1}H-NMR.

3 + $CoCp_2$

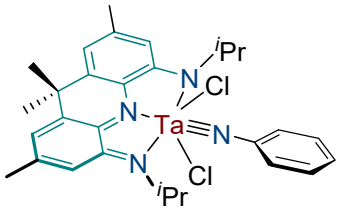

3

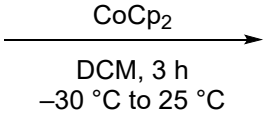

(unselective decomposition)

$CoCp_2$ (3.9 mg, 20.6 µmol, 0.95 eq.) is added into a J-Young flask and dissolved in DCM (2 mL), **3** (15 mg, 21.7 µmol, 1.0 eq.) is dissolved in a separate flask and added dropwise to the stirring $CoCp_2$ solution. After stirring the reaction mixture for 3 h at 25 °C the solvent is removed and re-dissolved in DCM-d_2. The ^{1}H-NMR shows unselective decomposition of the compound (See **Figure S26**).

3 + KC_8 in presence of 222-crypt

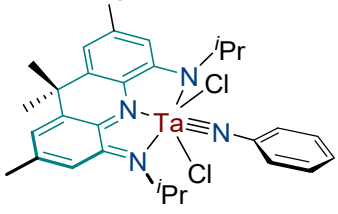

3

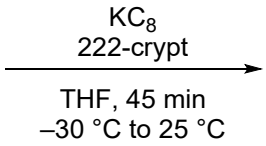

(unselective decomposition)

3 (20.0 mg, 28.9 µmol, 1 eq.) and 4,7,13,16,21,24-Hexaoxa-1,10-diazabicyclo[8.8.8]hexacosan (222-crypt) (10.9 mg, 28.9 µmol, 1 eq.) are dissolved in THF and cooled for 10 min to −30 °C. KC_8 is added to the stirring cold solution and slowly warmed to 25 °C. After stirring for 45 min the reaction solution is filtrated, the solvent removed under reduced pressure and re-dissolved in THF-d_8. The ^{1}H-NMR shows unselective decomposition the compound (See **Figure S27).**

3 + Brookhart's acid

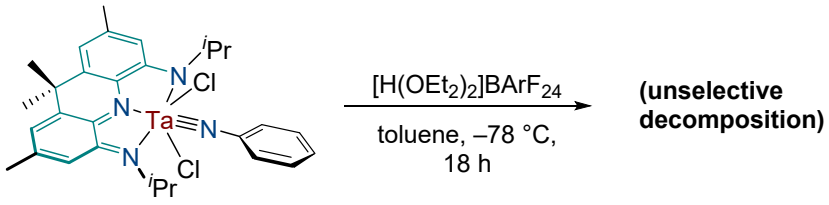

3

3 (20 mg, 28.9 µmol, 1.0 eq.) is added to J-Young flask and dissolved in toluene. $[H(OEt_2)_2][BArF_{24}]$ (29.3 mg, 28.9 µmol, 1.0 eq.) is dissolved in Et_2O in a separate Schlenk flask. The flask containing the Tantalum-complex is cooled to −78 °C for 5 min and the solution containing the Brookhart's acid is slowly added to the stirring cooled solution. After stirring for 15 min at −78 °C the reaction solution is slowly warmed to 25 °C. The solvent is removed under reduced pressure. The dark violet oil is washed with hexane (3 x 5 mL), residual solvent is removed under reduced pressure and the violet oil is re-dissolved in THF-d_8. The ^{1}H-NMR shows unselective decomposition of the compound (See **Figure S28**).

Spectroscopic Data (Synthesis and reactivity of Ta coordination compounds)
VT-NMR of complex I

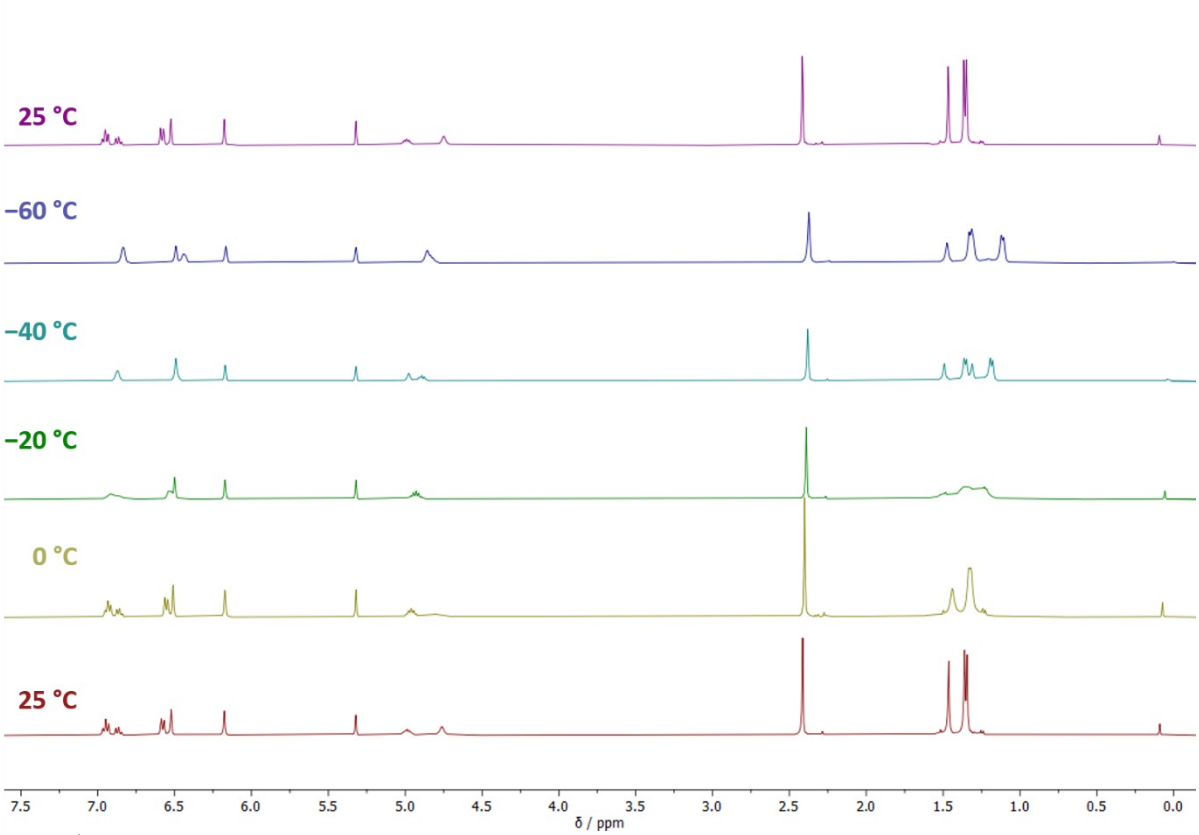

Figure S6. ^{1}H VT-NMR spectrum of **I** + 1 eq. of aniline, CD_2Cl_2, 25 °C to −60 °C.

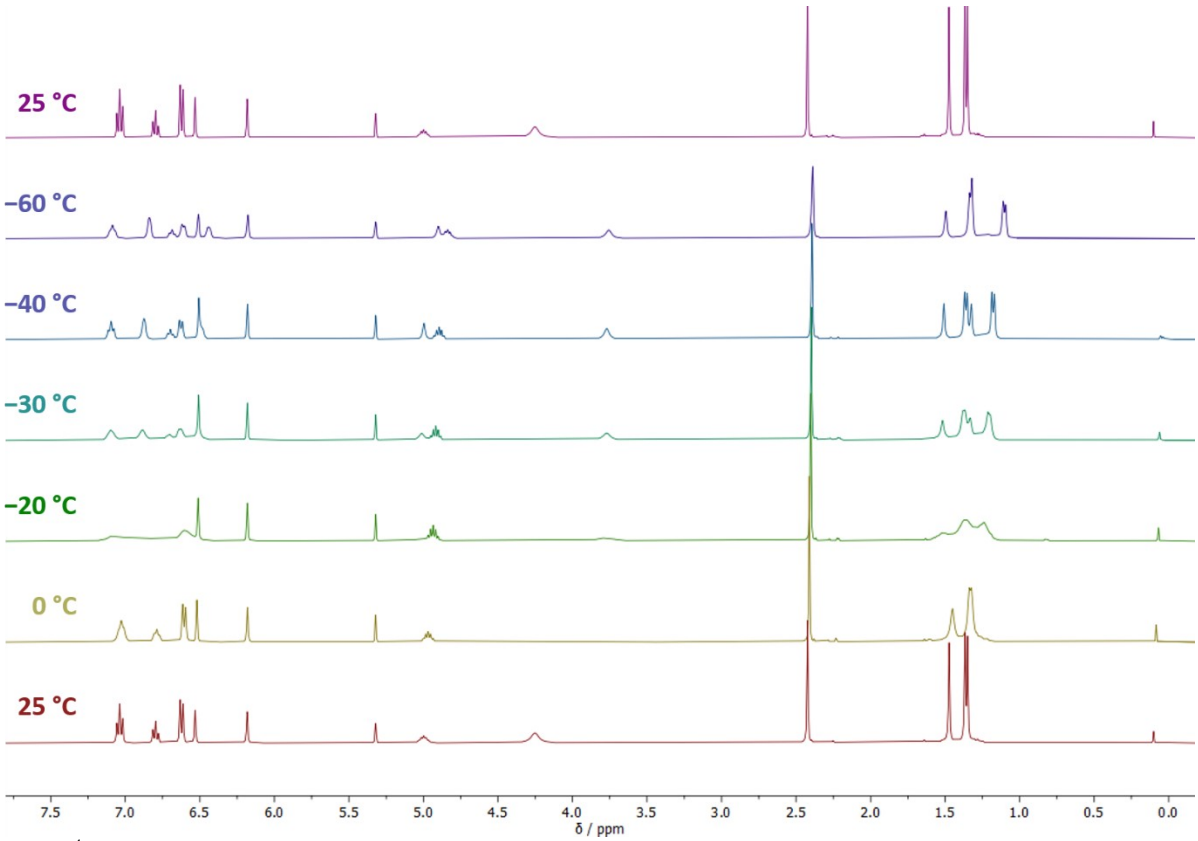

Figure S7. ^{1}H VT-NMR spectrum of **I** + 2 eq. of aniline, CD_2Cl_2, 25 °C to −60 °C.

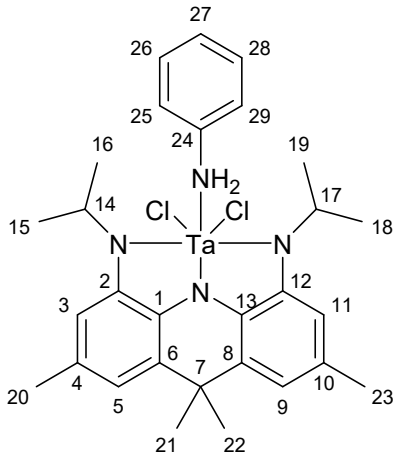

Scheme S2. Carbon numbering of **1** for clarification of NMR signal assignment. Assignment of the proton signals is conducted using the ^{1}H NMR at −40 °C showing the best peak separation as well as coupling.

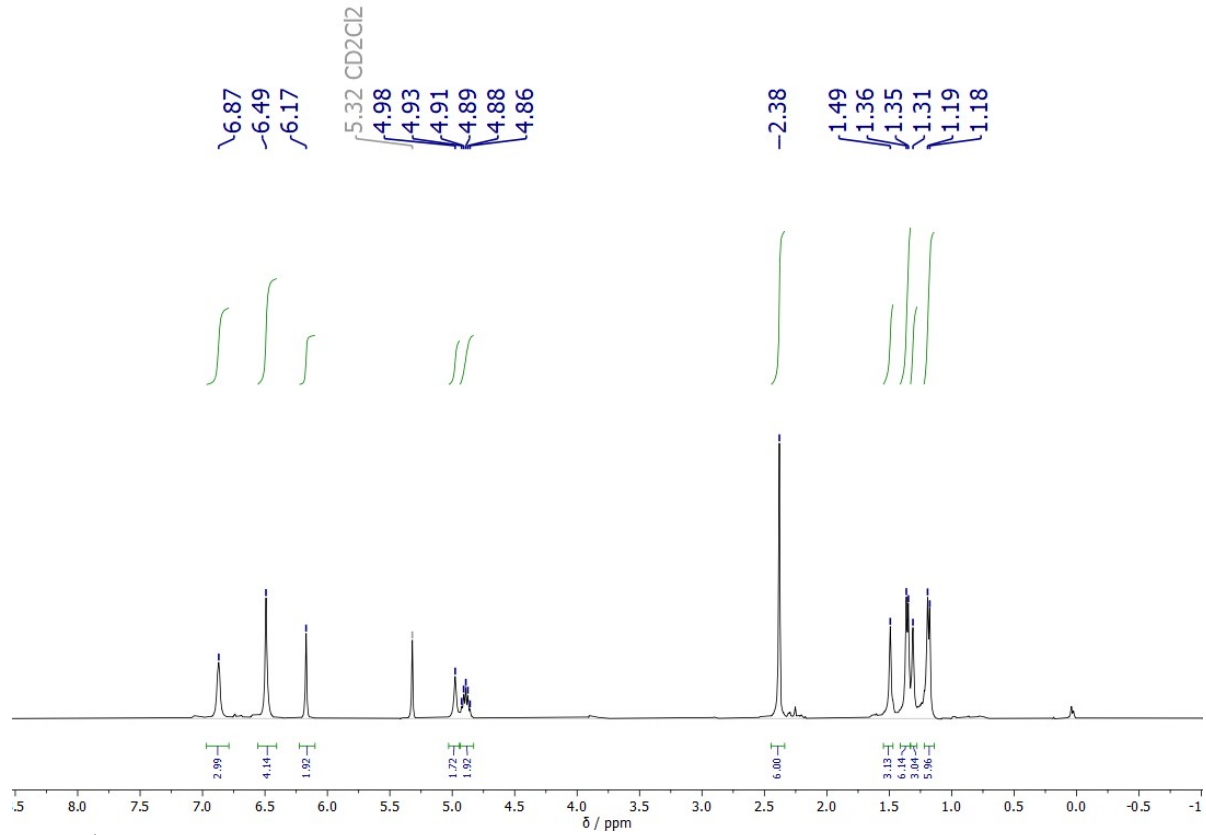

Figure S8. ^{1}H NMR spectrum of **1**, CD_2Cl_2, −40 °C.

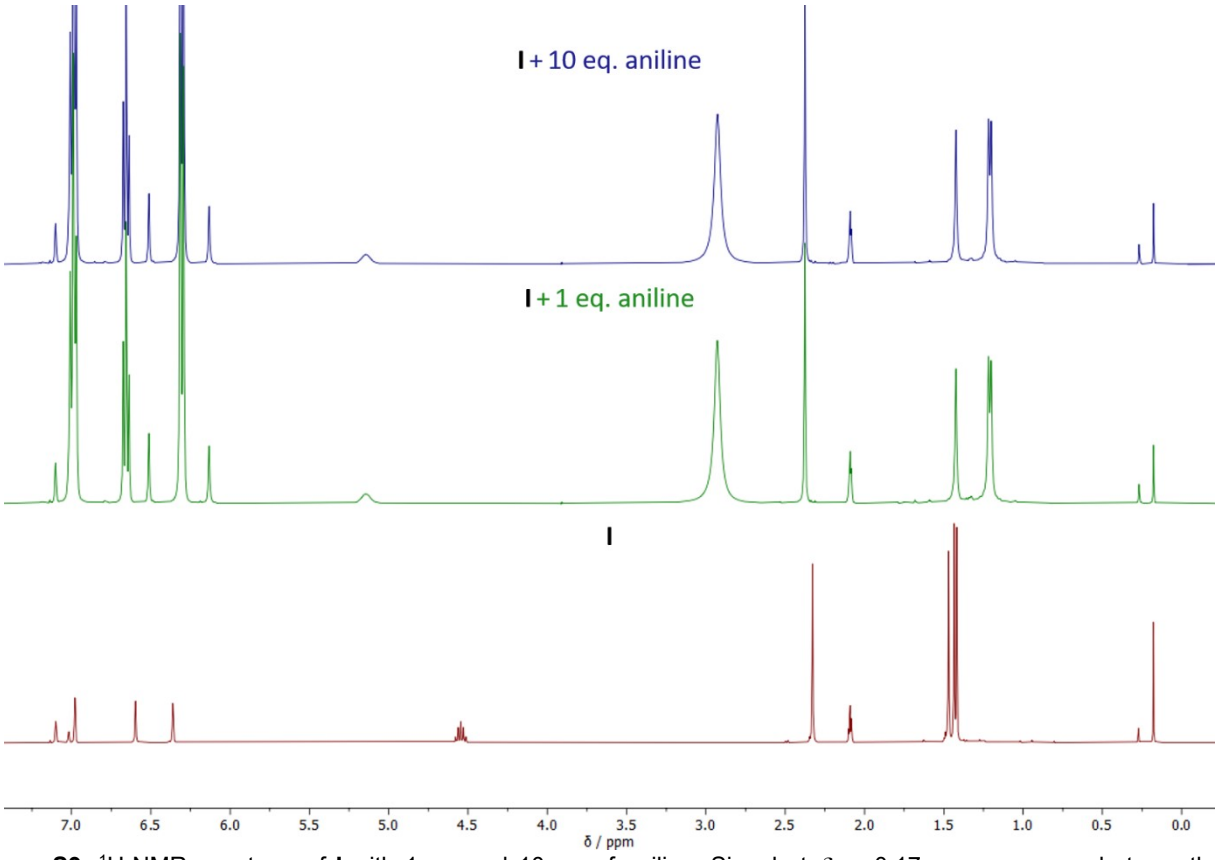

Figure S9. ^{1}H-NMR spectrum of **I** with 1 eq. and 10 eq. of aniline. Signal at δ_H = 0.17 ppm corresponds to methane originating from the freshly prepared solution of **I**, tol-d_8, 25 °C.

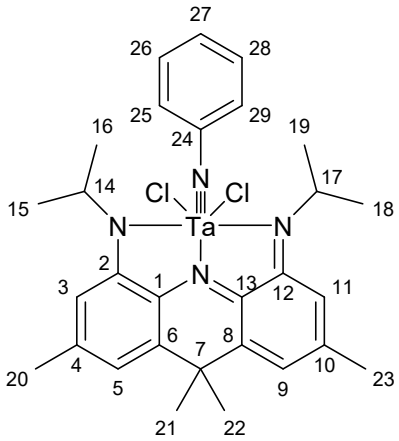

Scheme S3. Carbon numbering of **3** for clarification of NMR signal assignment. The experimental bond distances indicate that both arms of the NNN pincer ligand exhibit identical C–C and C–N bond lengths, preserving symmetry even upon one- or two-electron ligand-centred oxidation. To clearly illustrate the ligand-centred oxidation in the Ta complexes, we chose to represent the chemical structures with asymmetrical ligands, enhancing the visual communication of this feature to the reader.

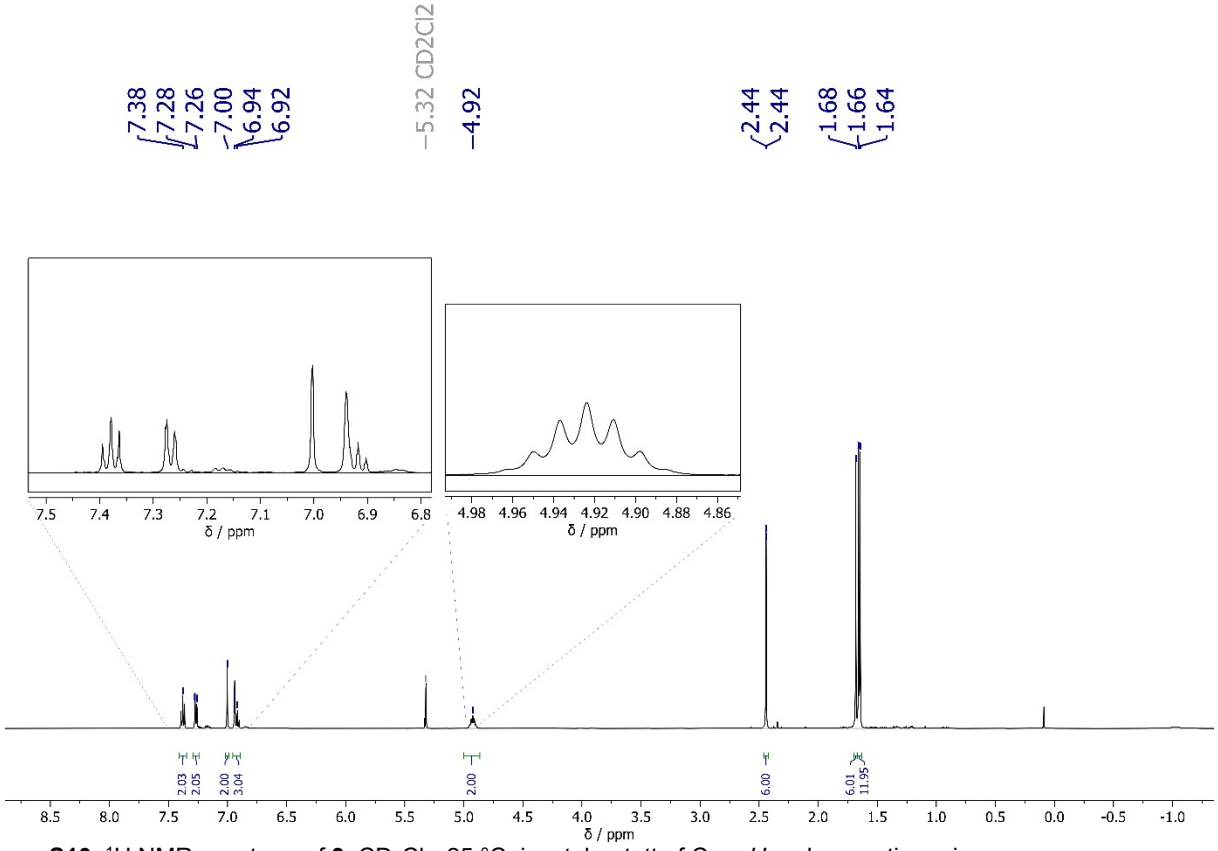

Figure S10. ^{1}H NMR spectrum of **3**, CD_2Cl_2, 25 °C, inset: heptett of $C_{14/17}H$ and aromatic region**.**

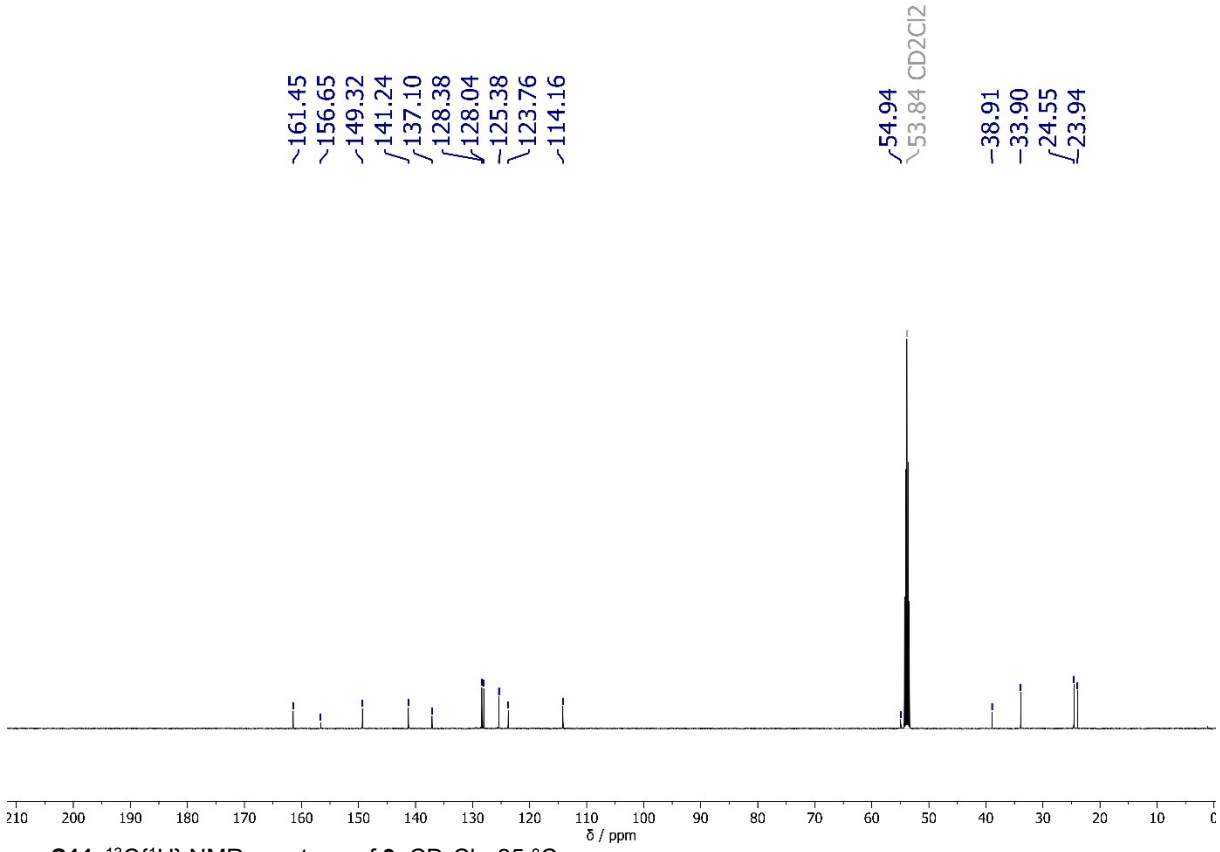

Figure S11. $^{13}C\{^{1}H\}$ NMR spectrum of **3**, CD_2Cl_2, 25 °C.

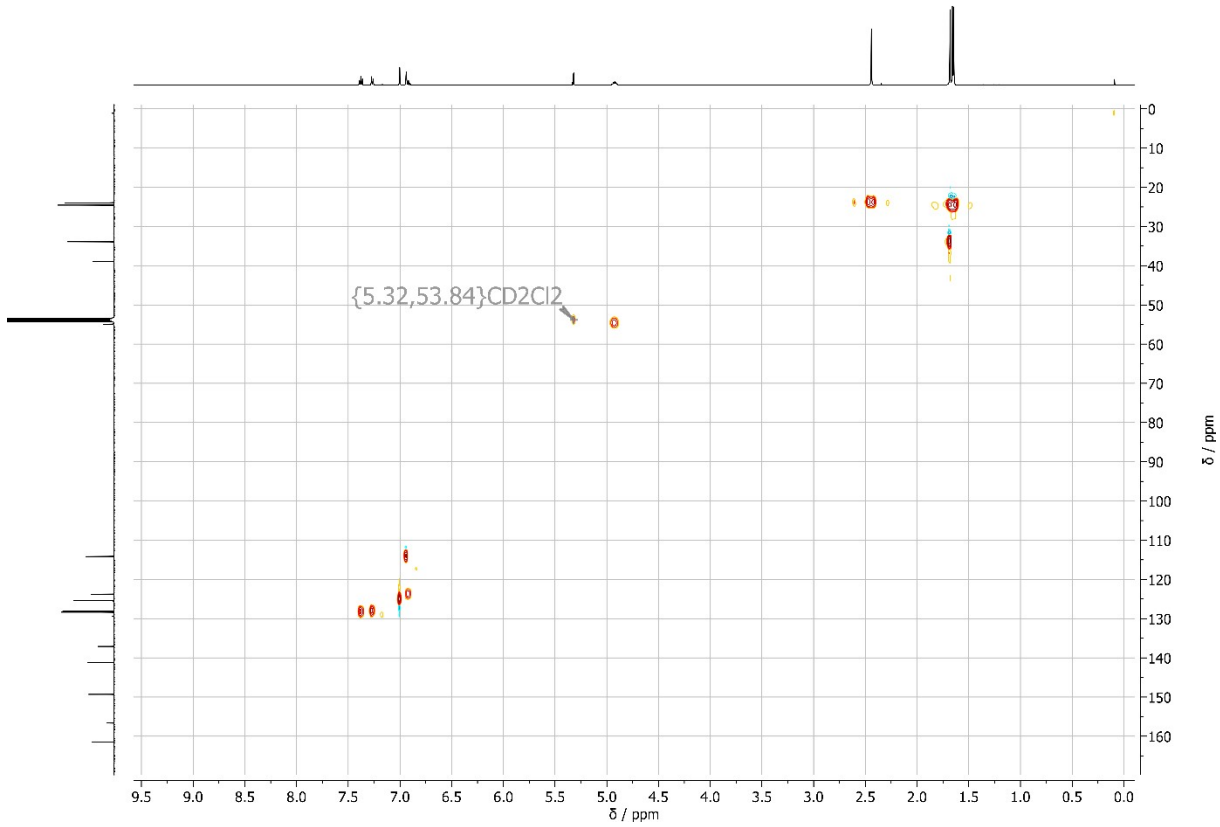

Figure S12. HSQC spectrum of **3**, CD_2Cl_2, 25 °C.

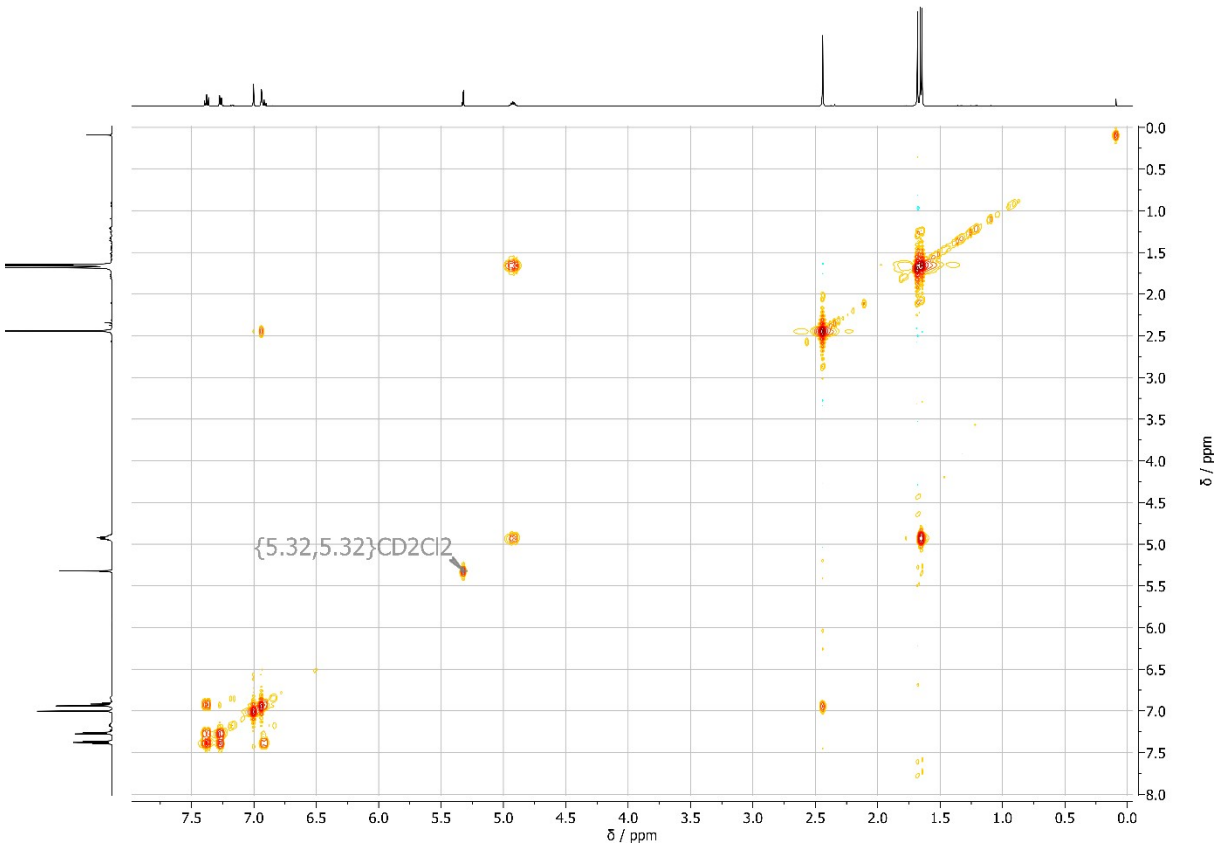

Figure S13. COSY spectrum of **3**, CD_2Cl_2, 25 °C.

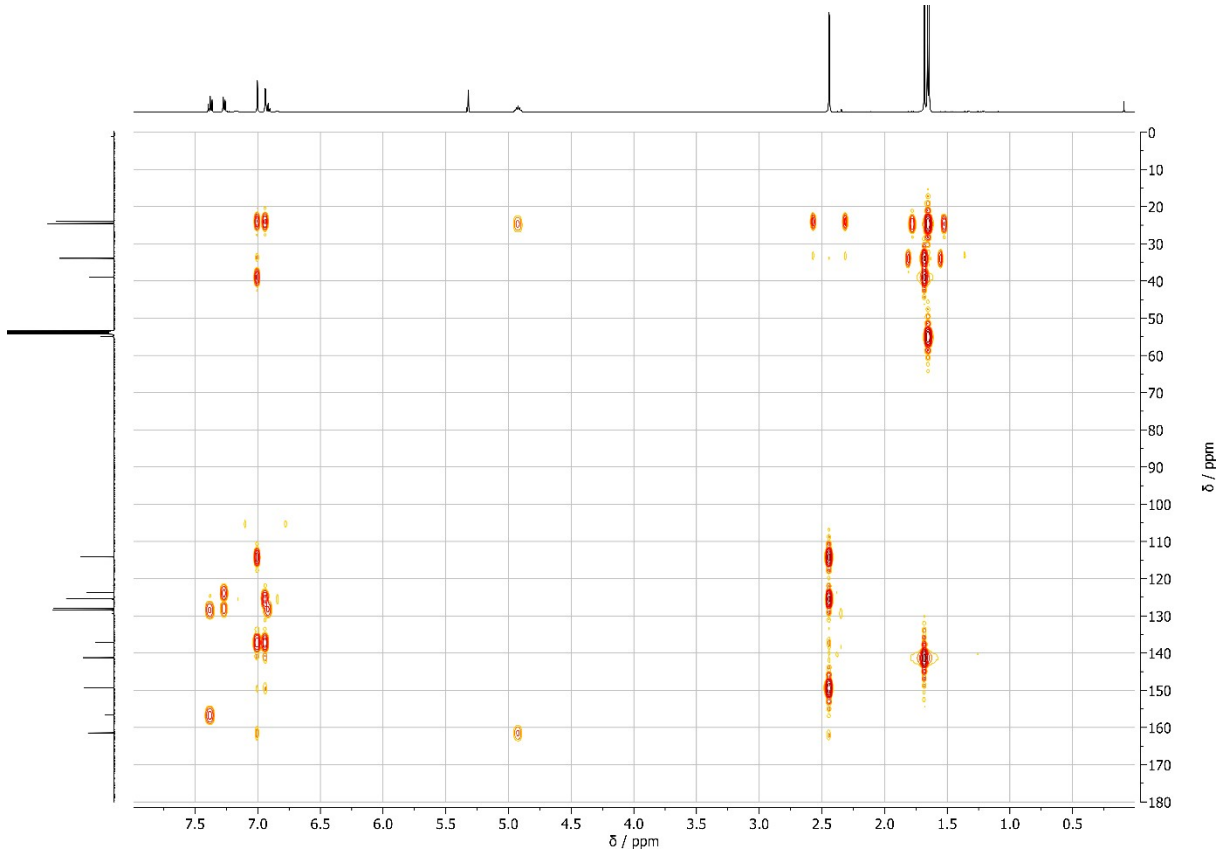

Figure S14. HMBC spectrum of **3**, CD_2Cl_2, 25 °C.

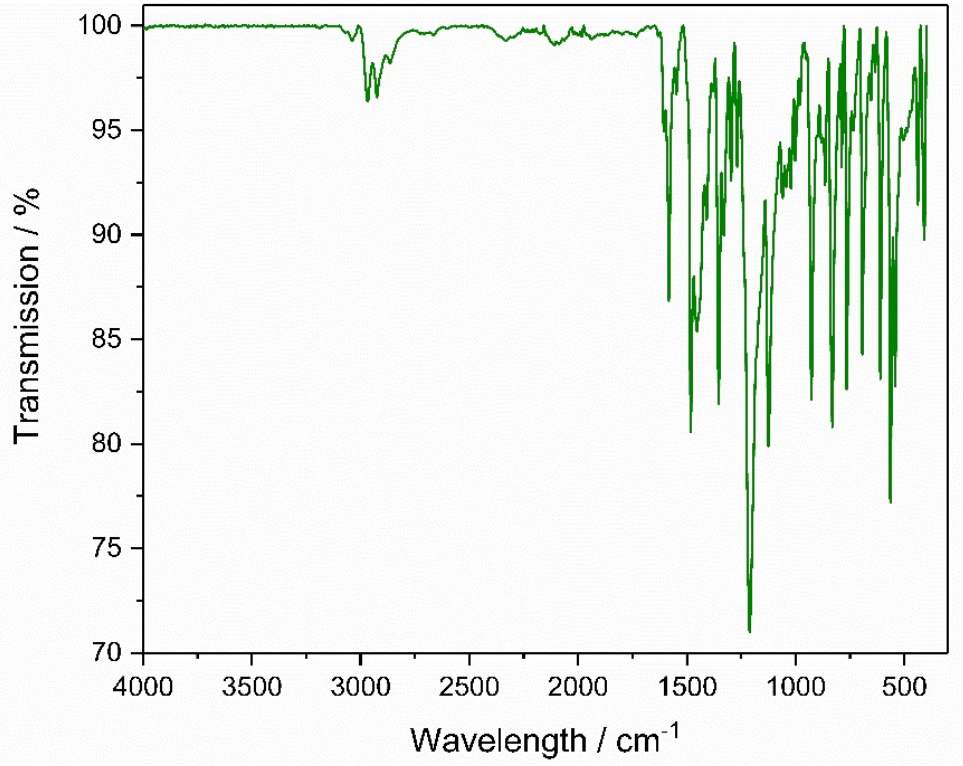

Figure S15. ATR-IR spectrum of **3**, solid, 25 °C.

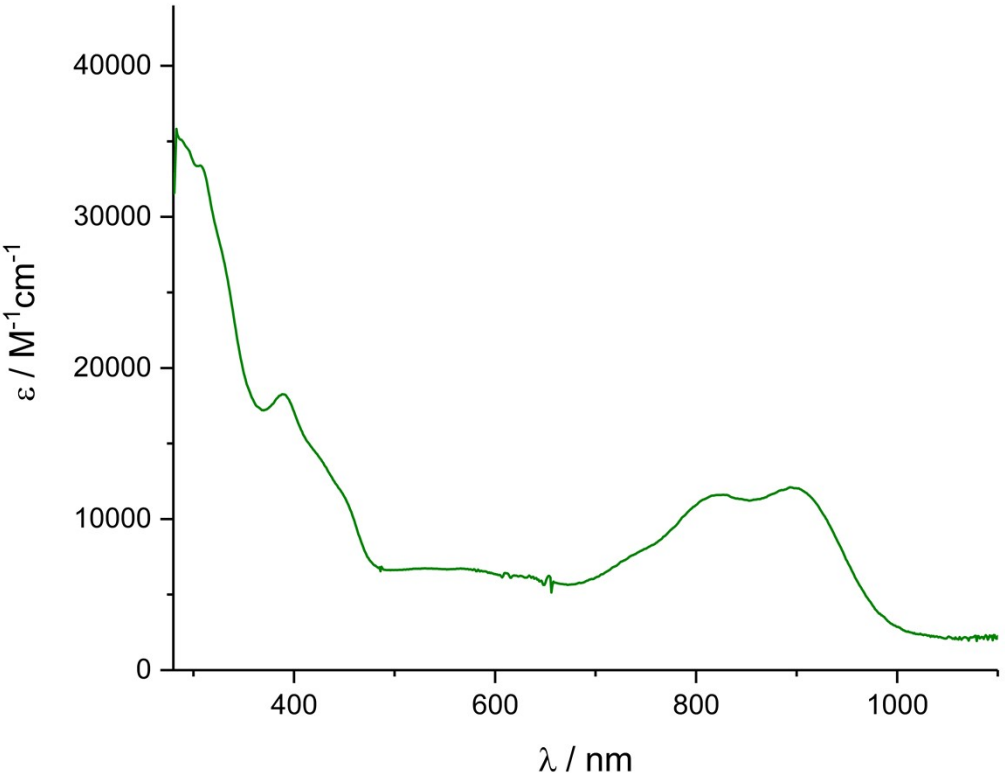

Figure S16. UV/vis spectrum of **3**, toluene, 25 °C.

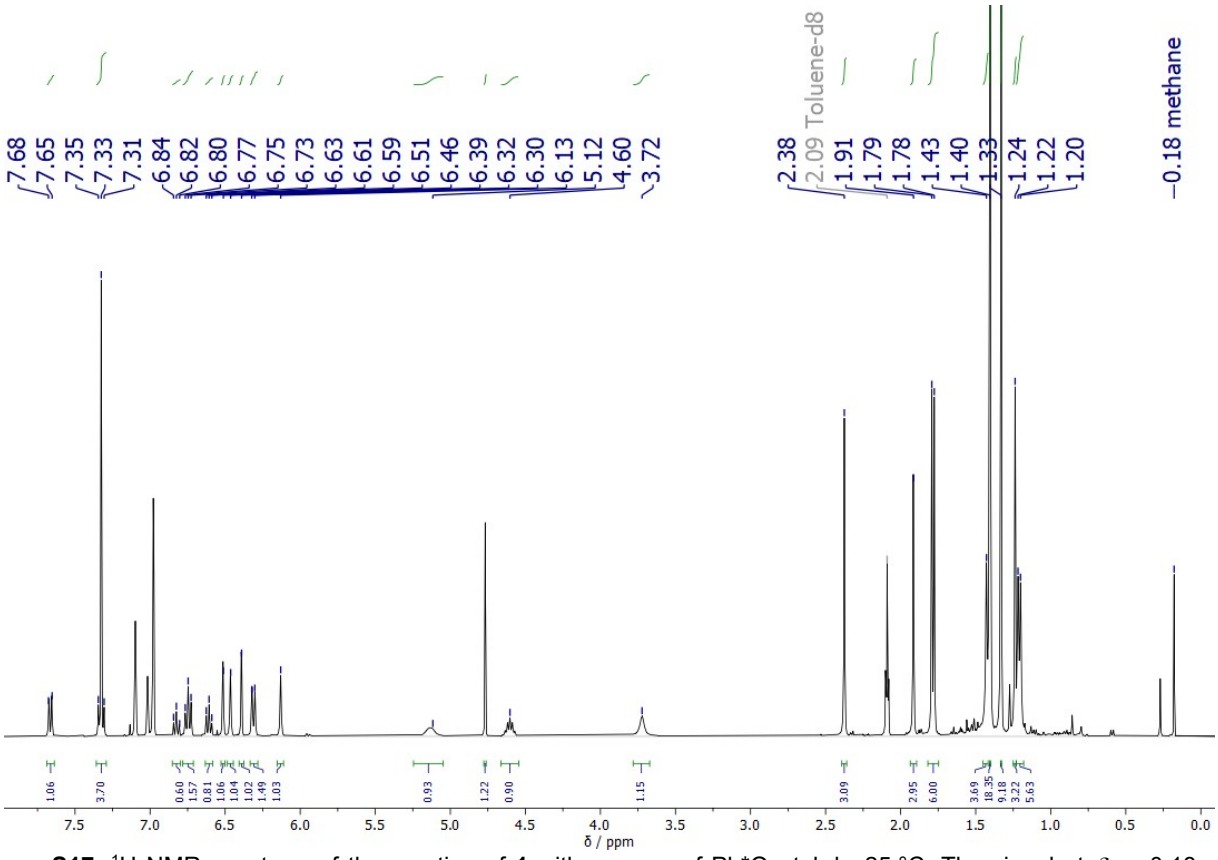

Figure S17. ^{1}H NMR spectrum of the reaction of **1** with one eq. of Ph*O·, tol-d_8, 25 °C. The signal at δ_H = 0.18 ppm corresponds to methane originating from the freshly prepared solution of **I**.

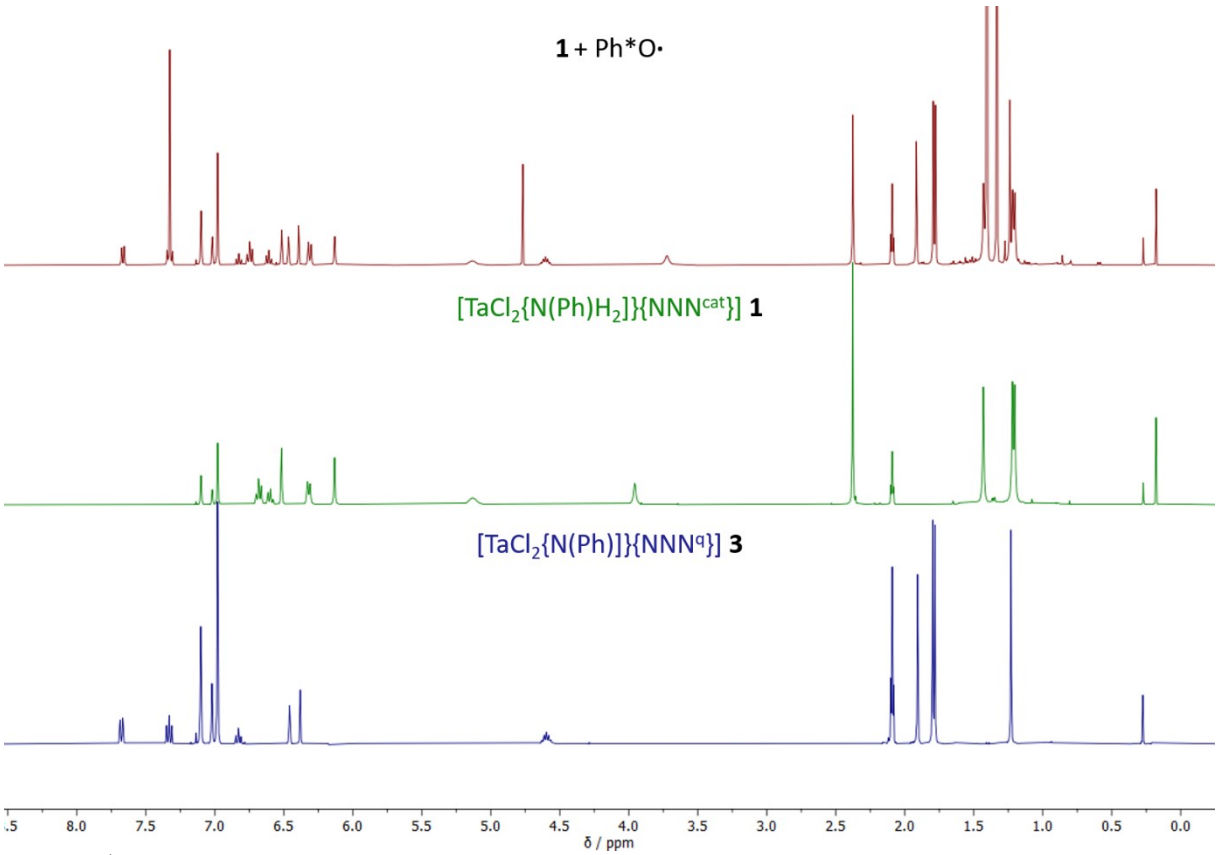

Figure S18. ^{1}H NMR spectrum of the reaction of **1** with one eq. of Ph*O·, tol-d_8, 25 °C and comparison with **3** and **1**. The signal at δ_H = 0.18 ppm corresponds to methane originating from the freshly prepared solution of **I**.

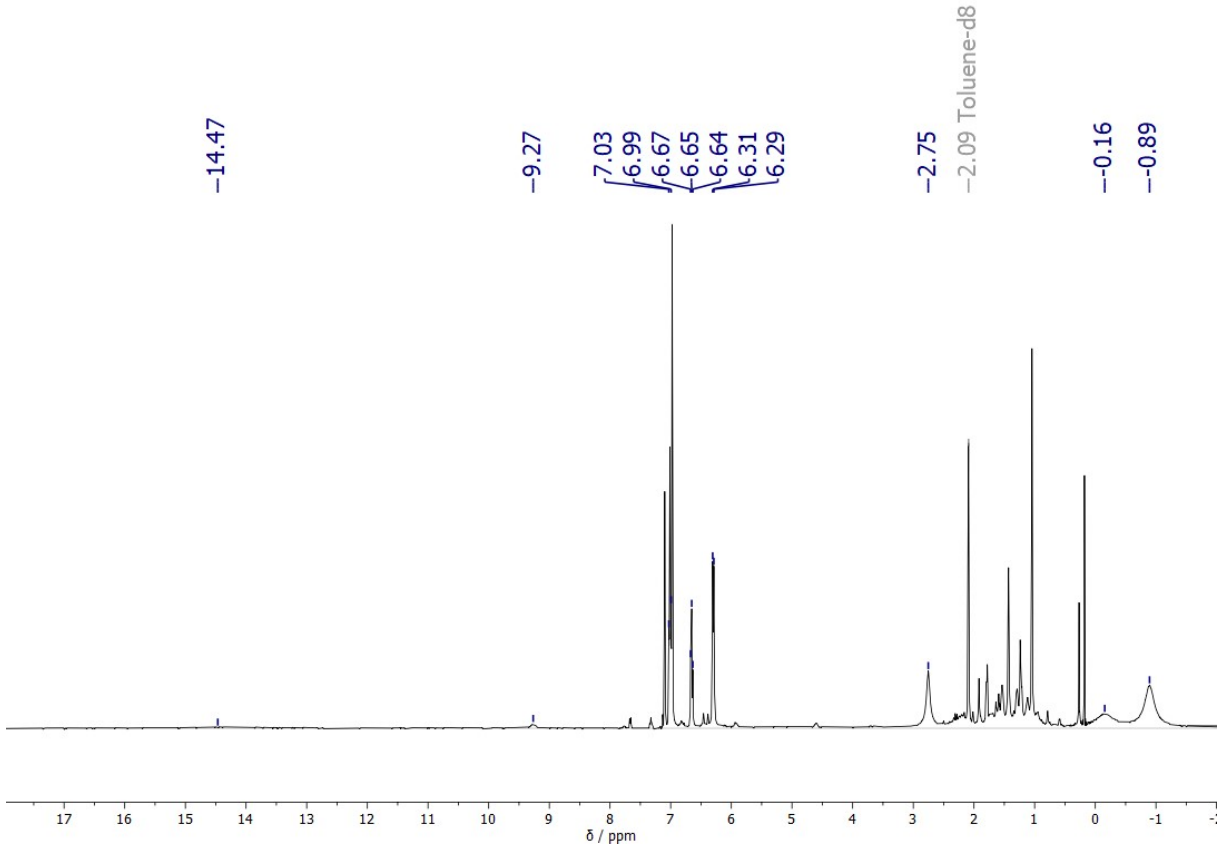

Figure S19. ^{1}H NMR spectrum of **1** reacting with TEMPO, tol-d8, 25 °C, free aniline can be detected at δ_H = 2.75, 6.65 – 6.29 ppm; indicative signals of **II** are detected at δ_H = –0.16 and –0.89 ppm.

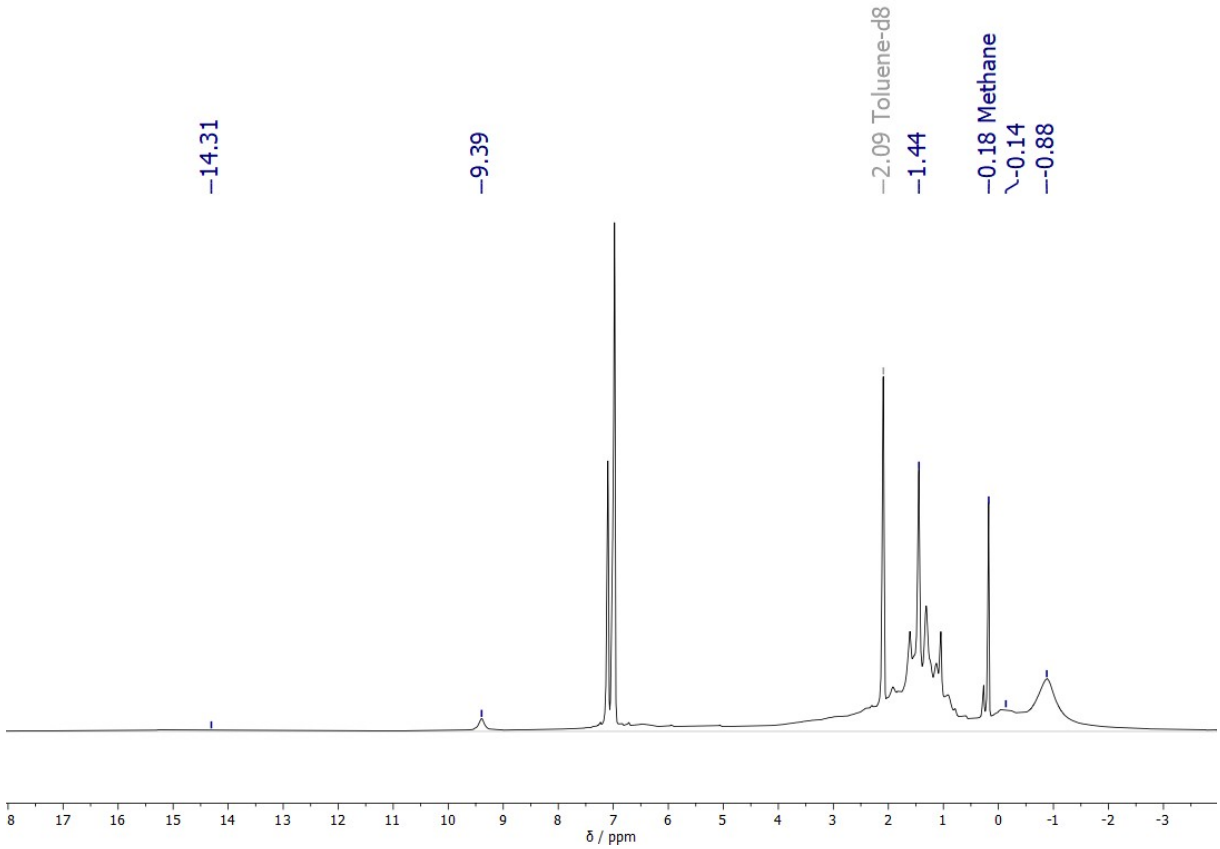

Figure S20. ^{1}H NMR spectrum of **I** reacting with TEMPO, tol-d8, 25 °C; **II** is detected at δ_H = –0.14 and –0.89 ppm.

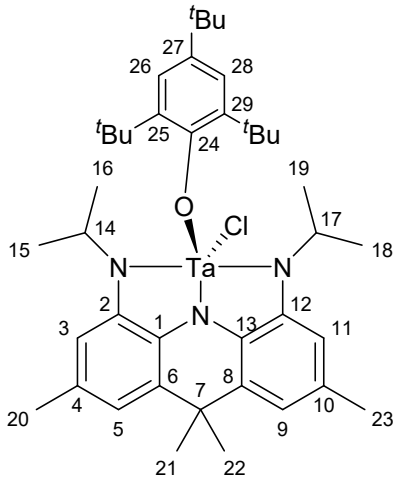

Scheme S4. Carbon numbering of **4** for clarification of NMR signal assignment.

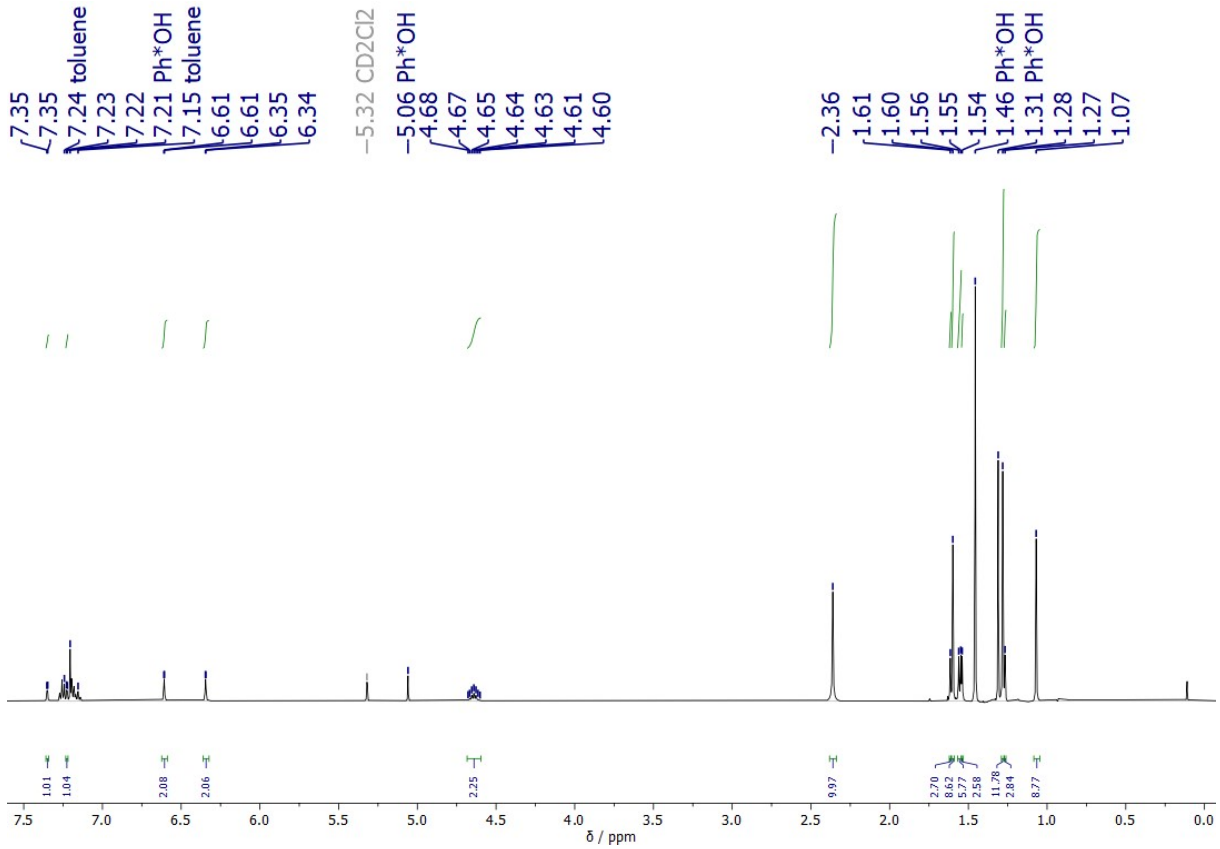

Figure S21. ^{1}H NMR spectrum of the reaction of **I** with PhO* producing **4** and Ph*OH, CD_2Cl_2, 25 °C**.**

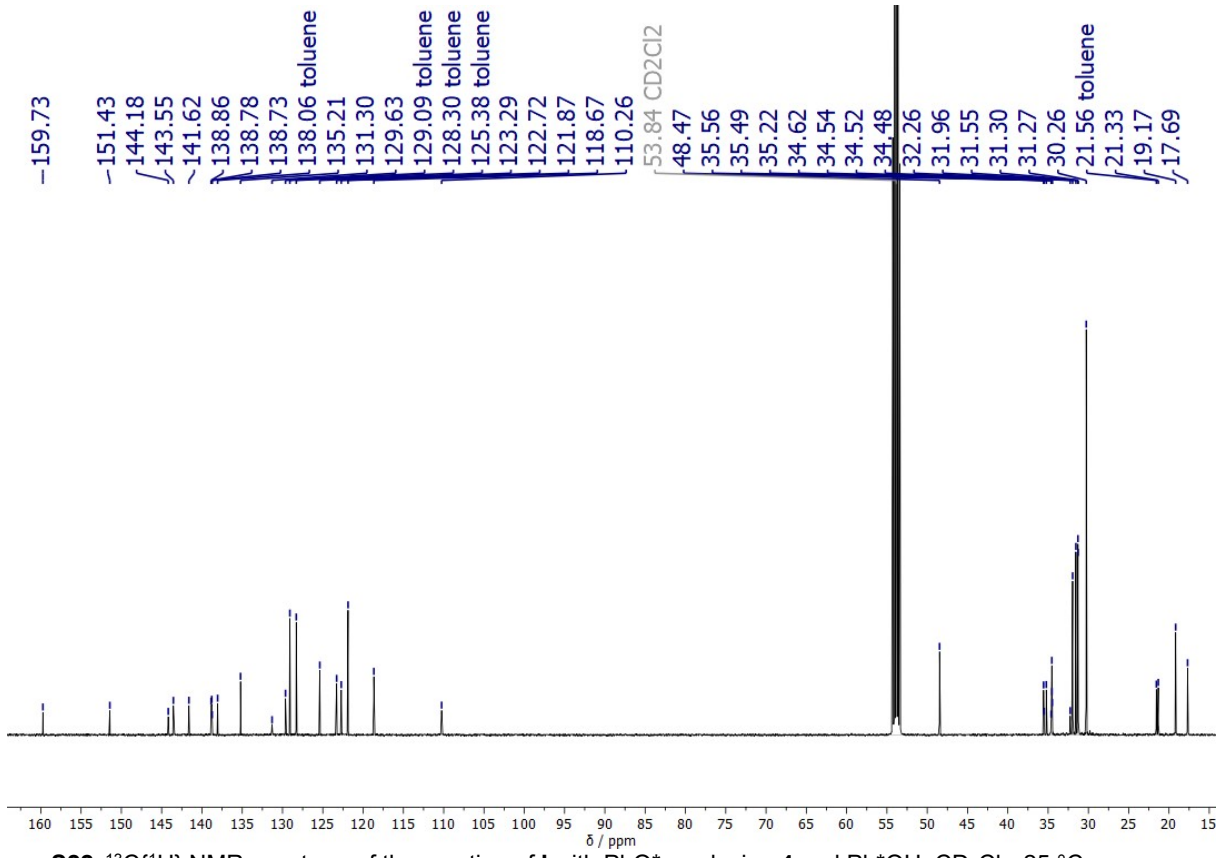

Figure S22. $^{13}C\{^{1}H\}$ NMR spectrum of the reaction of **I** with PhO* producing **4** and Ph*OH, CD_2Cl_2, 25 °C.

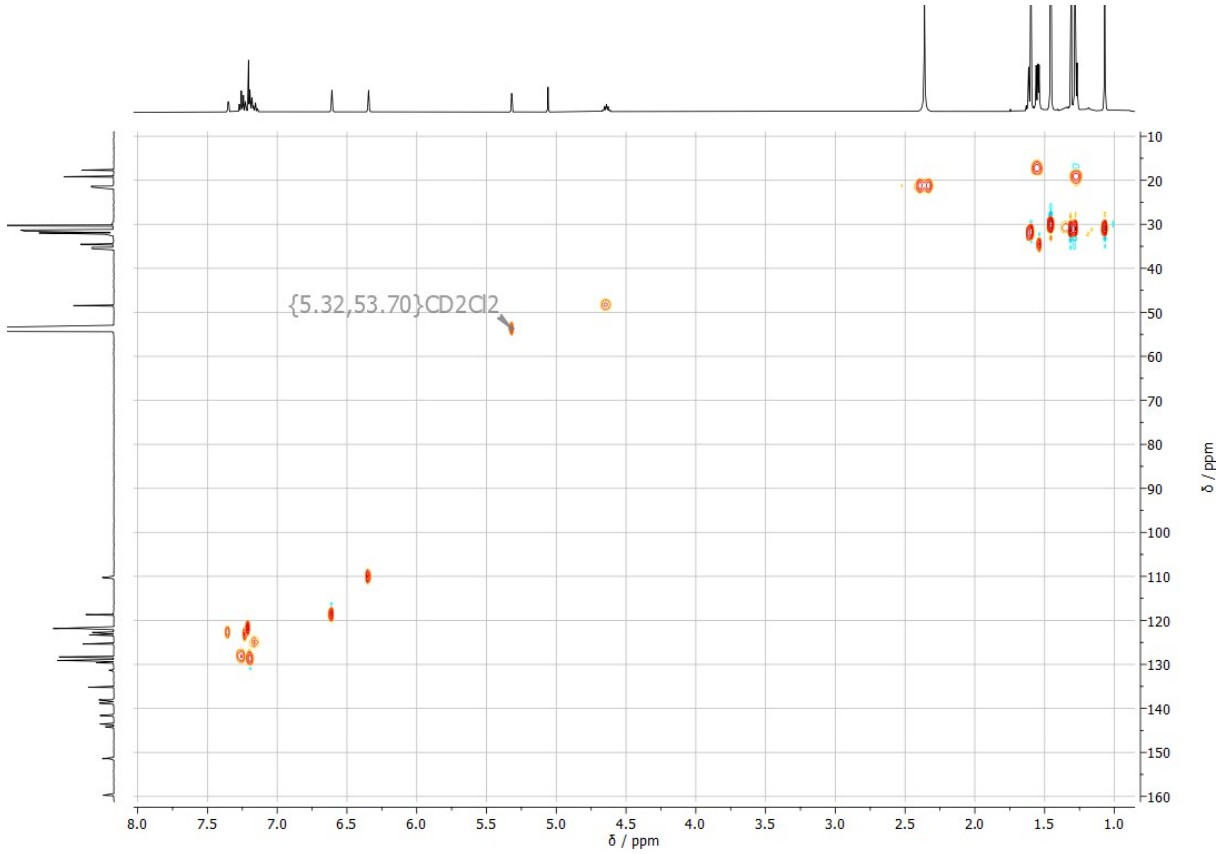

Figure S23. HSQC spectrum of the reaction of **I** with PhO* producing **4** and Ph*OH, CD_2Cl_2, 25 °C.

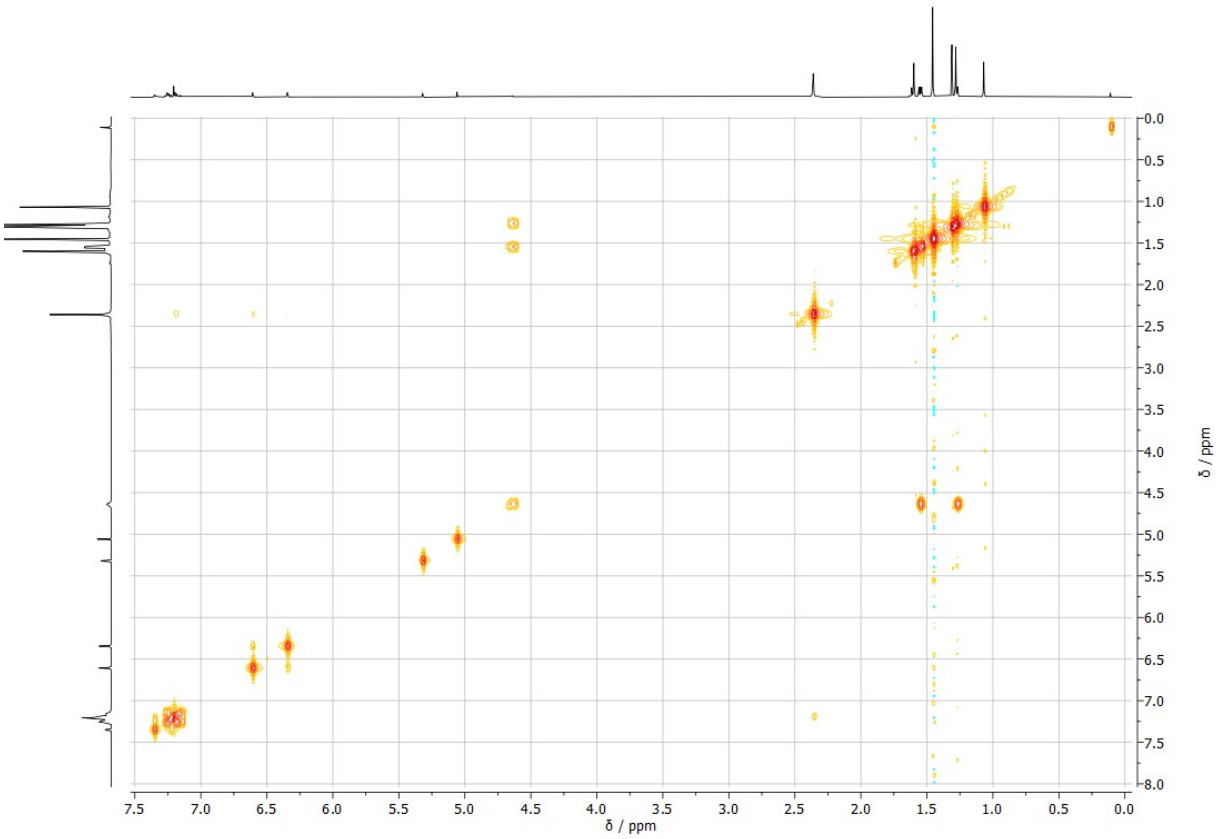

Figure S24. COSY spectrum of the reaction of **I** with PhO* producing **4** and Ph*OH, CD_2Cl_2, 25 °C.

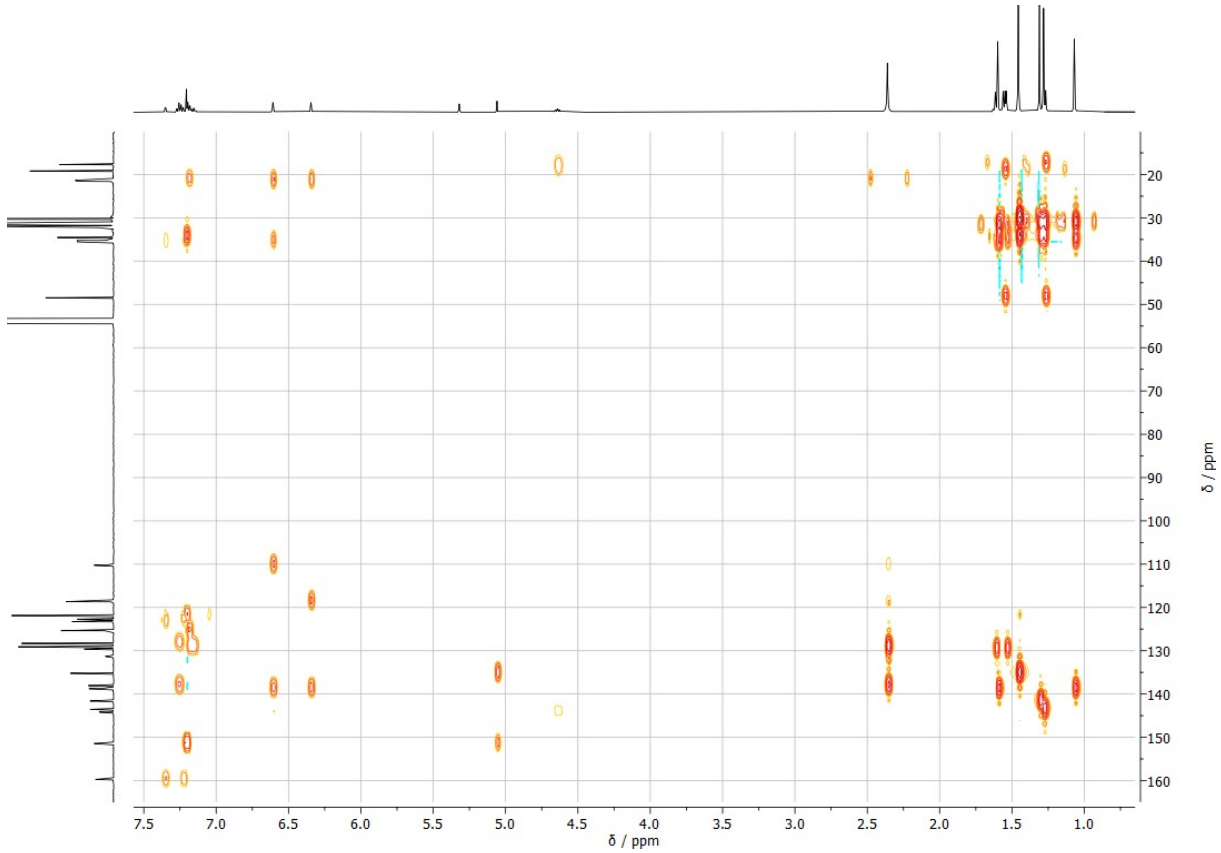

Figure S25. HMBC spectrum of the reaction of **I** with PhO* producing **4** and Ph*OH, CD_2Cl_2, 25 °C.

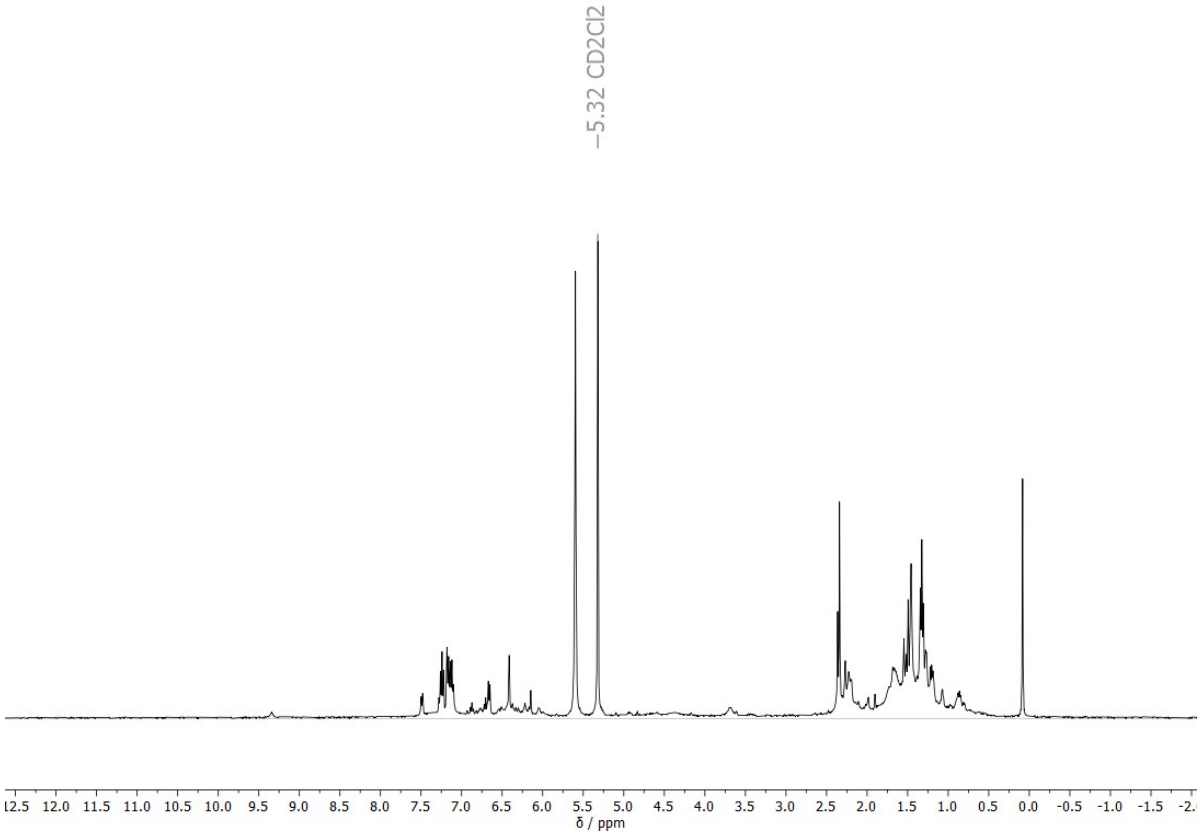

Figure S26. ^{1}H-NMR spectrum of **3** + $CoCp_2$, CD_2Cl_2, 25 °C; no paramagnetic complex was detected. Partial precipitation of $[CoCp_2]Cl$ (evidenced by its colour) indicates unselective decomposition.

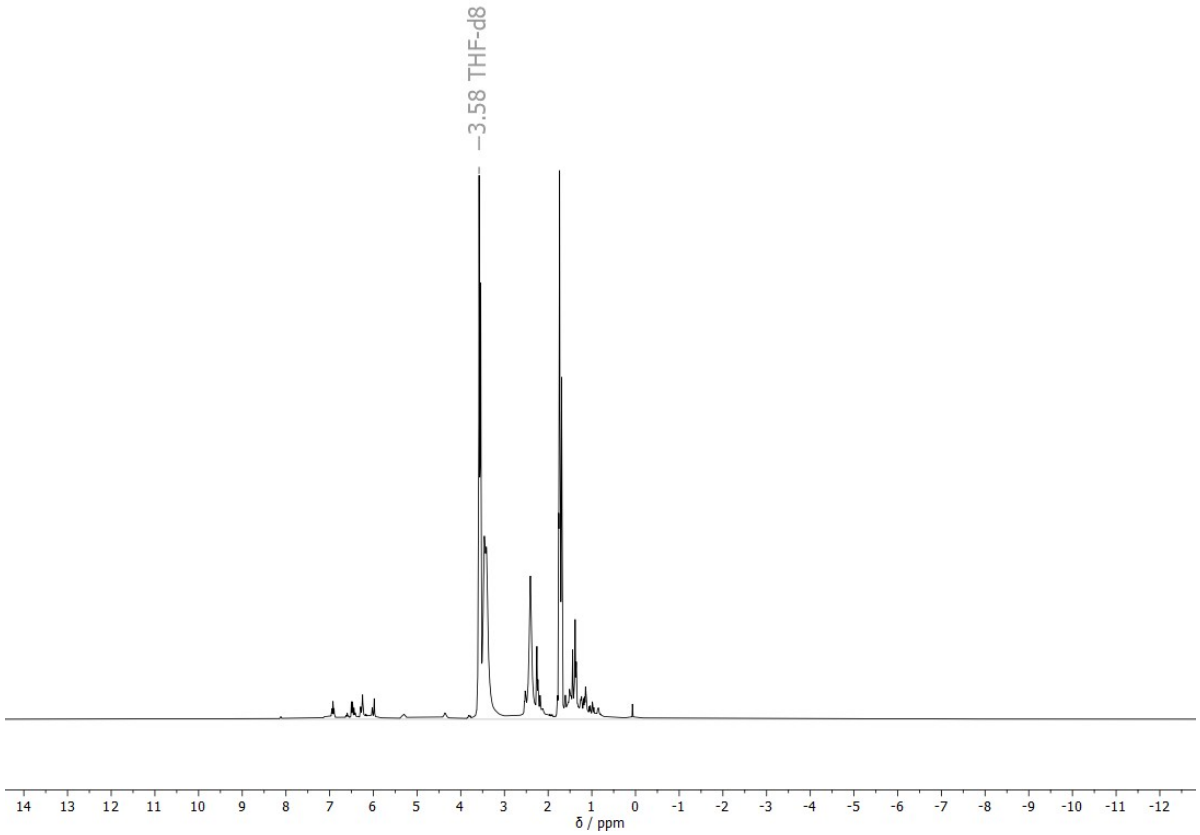

Figure S27. ^{1}H-NMR spectrum of **3** + KC_8, THF-d_8, 25 °C; no paramagnetic complex was detected.

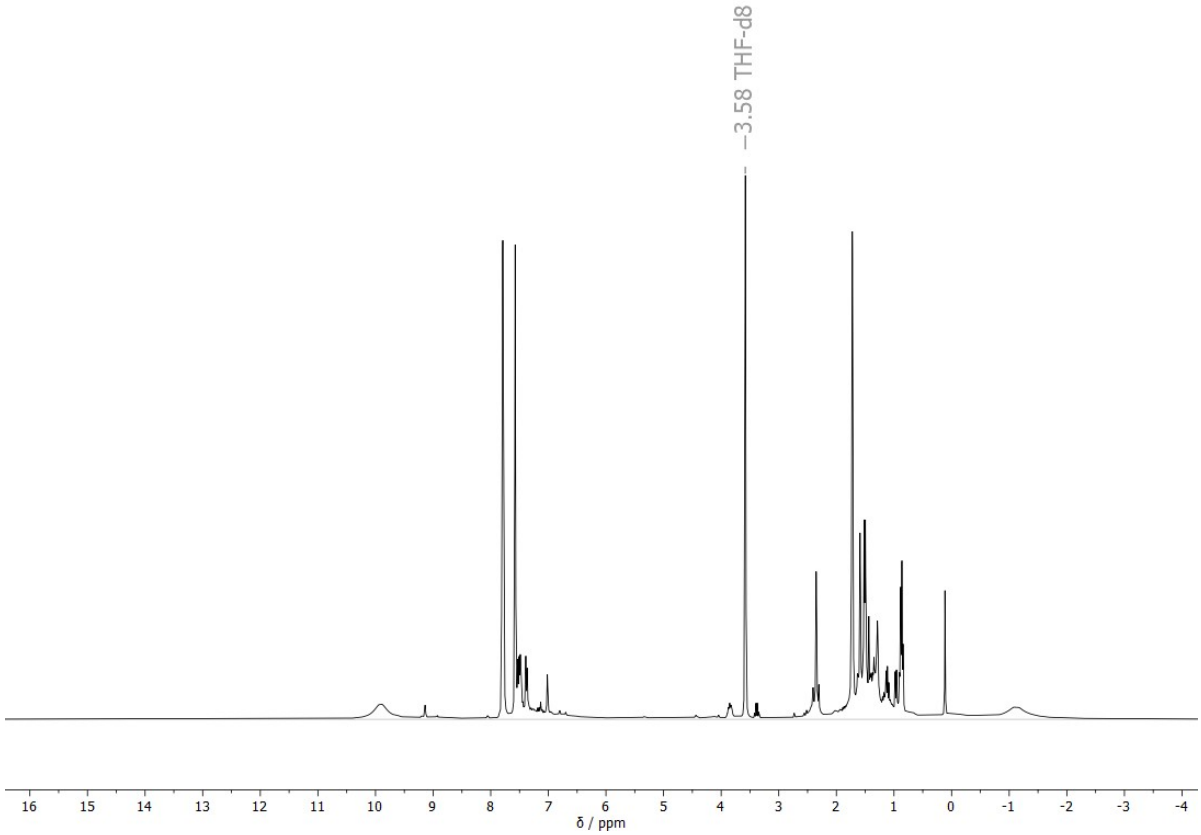

Figure S28. ^{1}H-NMR spectrum of **3** + $[H(OEt_2)_2][BArF_{24}]$, THF-d_8, 25 °C.

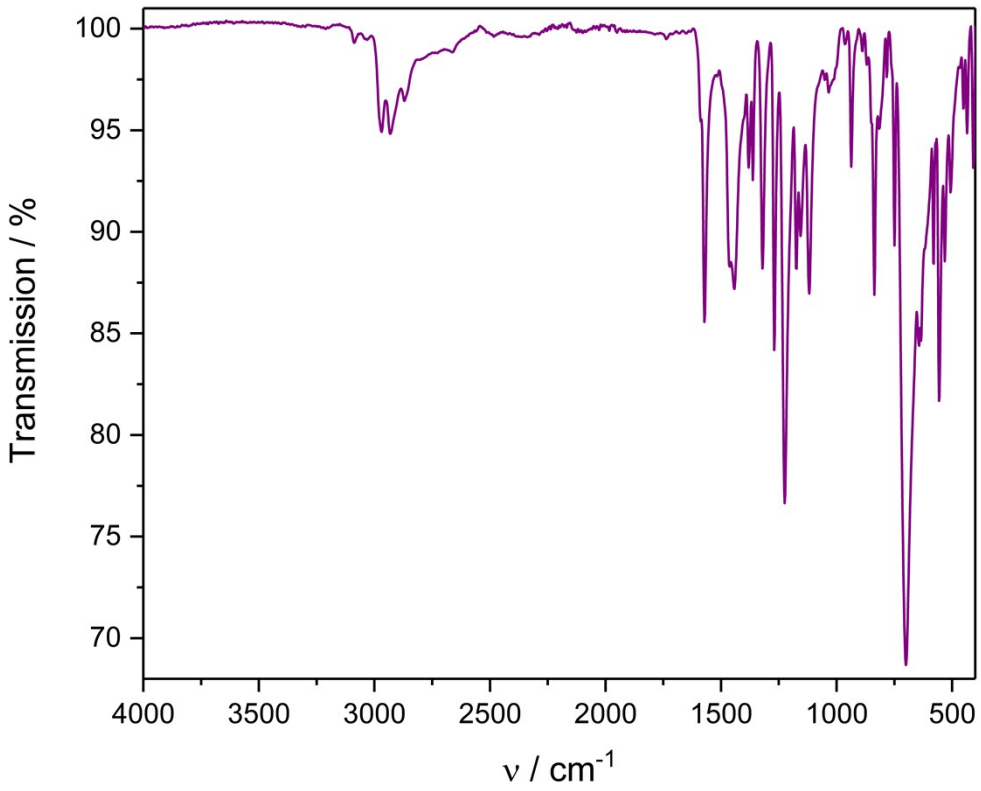

Figure S31. ATR-IR spectrum of **5**, solid, 25 °C.

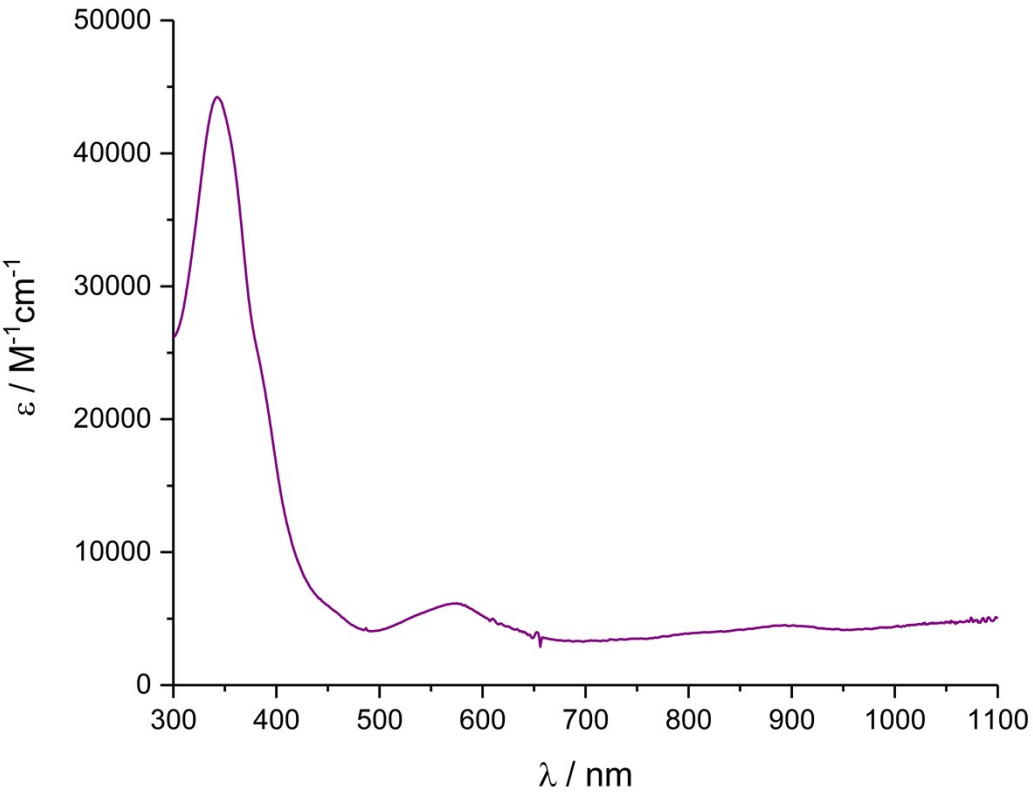

Figure S32. UV/vis spectrum of **5,** toluene, 25 °C.

Cyclic Voltammetry

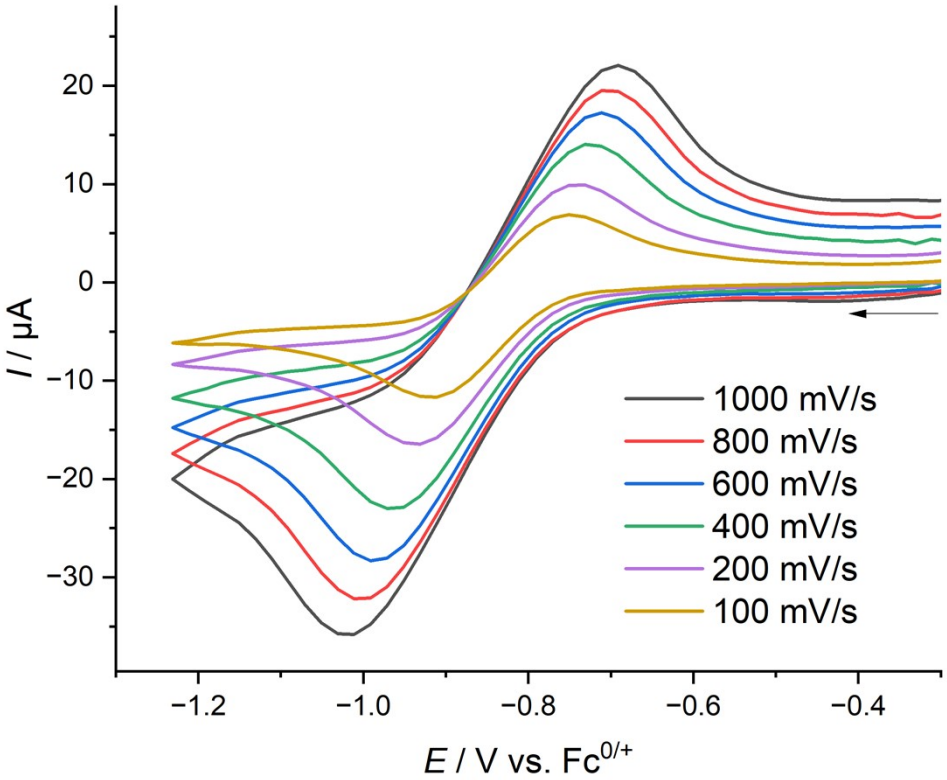

Figure S33. Cyclic voltammogram of **3**, THF; 25 °C, 0.1 M $[NBu_4][PF_6]$, 1 mM **3**.

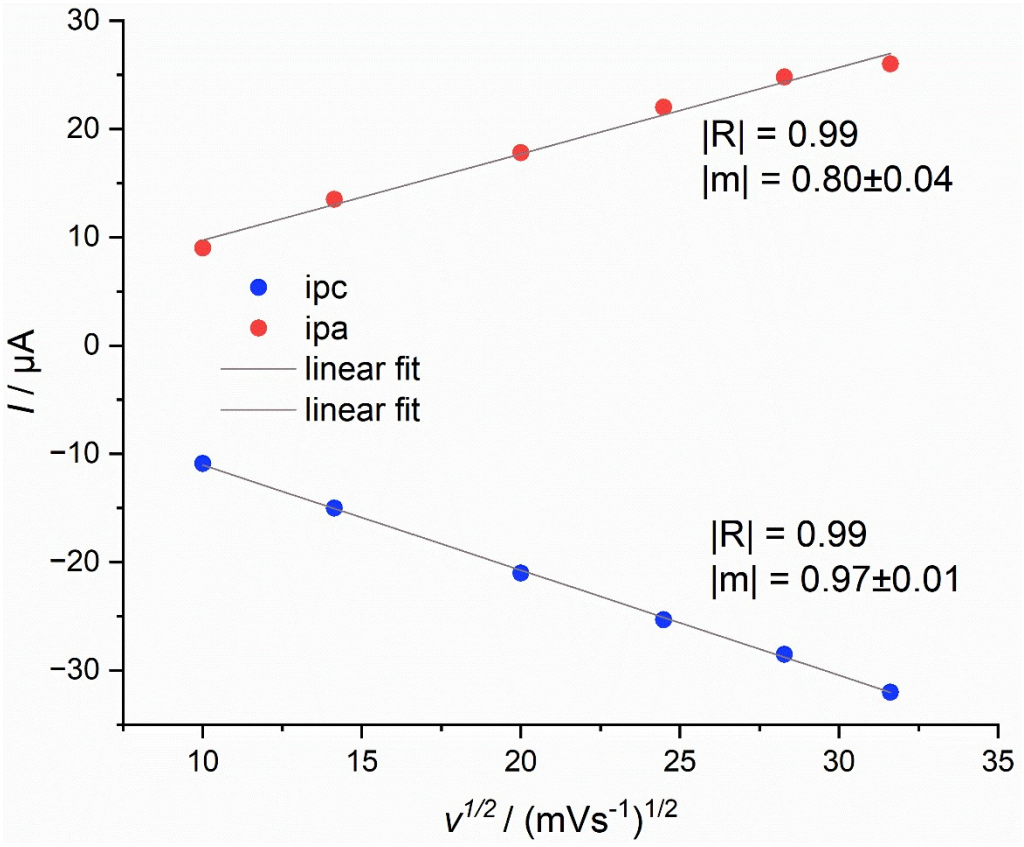

Figure S34. Peak current of the first redox event plotted against the square root of the scan rate including their linear fits. Fully reversible electron transfer between the analyte and the electrode is evident.

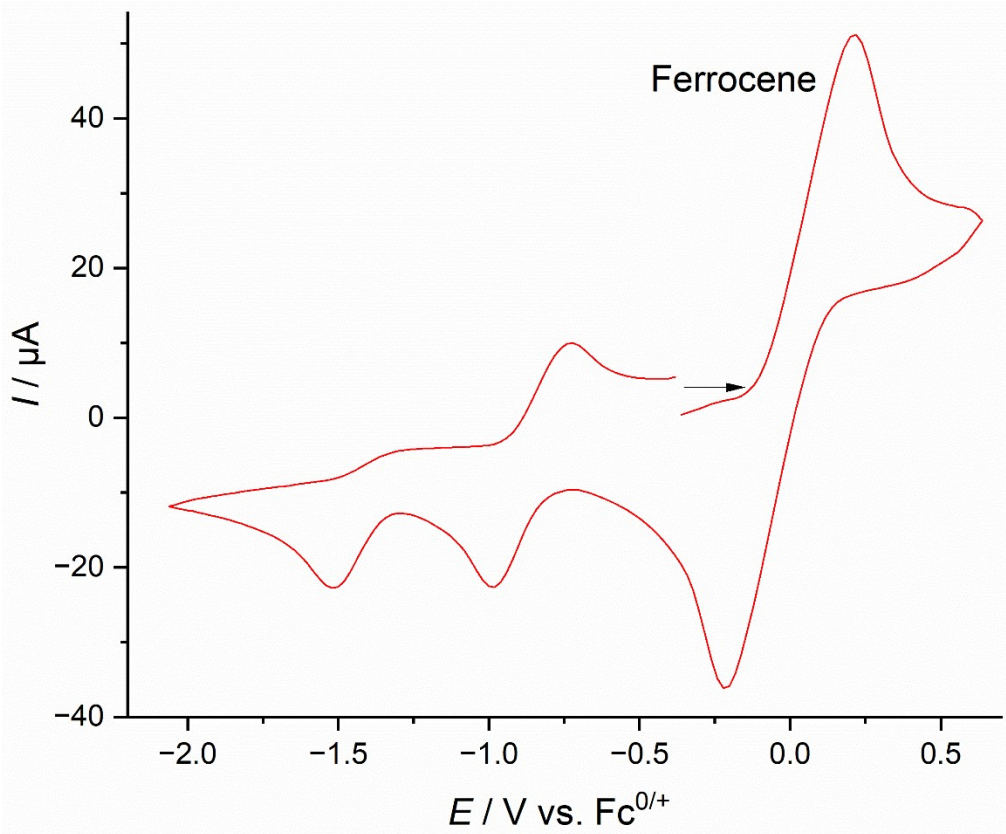

Figure S35. Cyclic voltammogram of **3** with ferrocene as internal reference showing a second fully irreversible redox event at $E \approx -1.4$ V vs $Fc^{0/+}$, THF; 25 °C, 0.1 M $[NBu_4][PF_6]$, 1 mM **3**, v = 400 mV/s.

Table S1. i_{pc}/i_{pa} ratios for the first reduction of **3** at different scan rates indicating the presence of a quasi-reversible reductive event. The data for higher scan rates is perturbed by the second irreversible redox event. The data point at v = 100 mV/s however clearly demonstrates the inequivalence of forward and backward peak currents.

Scan rate (mV/s)	i_{pc}/i_{pa}
1000	−1.23
800	−1.15
600	−1.15
400	−1.18
200	−1.11
100	–1.21

Single Crystal X-ray Diffraction
Crystallographic details of 3

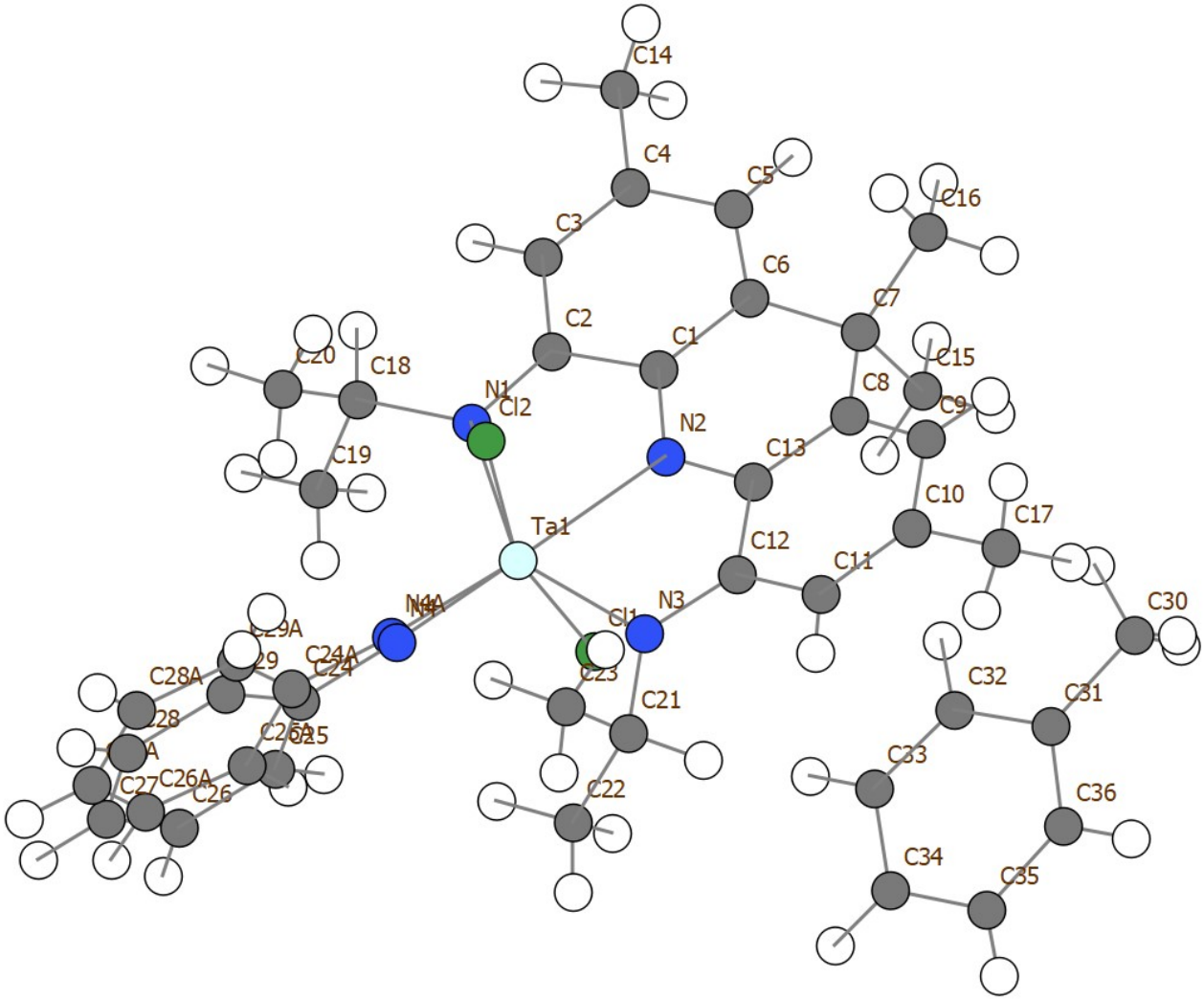

A purple, block-shaped crystal of mo_ja24_sp_ii_61_2_0m_a (**3**) was mounted on a MiTeGen micromount with perfluoroether oil. Data were collected from a shock-cooled single crystal at 100(2) K on a Bruker D8 VENTURE dual wavelength Mo/Cu three-circle diffractometer with a microfocus sealed X-ray tube using a mirror optics as monochromator and a Bruker PHOTON III detector. The diffractometer was equipped with an Oxford Cryostream 800 low temperature device and used MoK_α radiation (λ = 0.71073 Å). All data were integrated with SAINT and a multi-scan absorption correction using SADABS was applied.[12,13] The structure was solved by direct methods using SHELXT and refined by full-matrix least-squares methods against F^2 by SHELXL-2019/2.[14,15] All non-hydrogen atoms were refined with anisotropic displacement parameters. All hydrogen atoms were refined isotropic on calculated positions using a riding model with their U_{iso} values constrained to 1.5 times the U_{eq} of their pivot atoms for terminal sp^3 carbon atoms and 1.2 times for all other carbon atoms. Disordered moieties were refined using bond lengths restraints and displacement parameter restraints. The largest residuals are not near the heavy atom or in chemically sensible positions. This is most probably due to slight twinning or other effects. Crystallographic data for the structures reported here have been deposited with the Cambridge Crystallographic Data Centre.[16] CCDC 2383359 contain the supplementary crystallographic data for this paper. These data can be obtained free of charge from The Cambridge Crystallographic Data Centre via www.ccdc.cam.ac.uk/structures. This report and the CIF file were generated using FinalCif.[17]

Table S2. Crystal data and structure refinement for mo_ja24_sp_ii_61_2_0m_a (**3**).

CCDC number	2383359
Empirical formula	$C_{65}H_{78}Cl_4N_8Ta_2$
Formula weight	1475.05
Temperature [K]	100(2)
Crystal system	monoclinic
Space group (number)	$P2_1/n$ (14)
a [Å]	16.6831(8)
b [Å]	10.0197(4)
c [Å]	18.8593(10)
α [°]	90
β [°]	98.358(2)
γ [°]	90
Volume [Å^3]	3119.0(3)
Z	2
ρ_{calc} [gcm^{-3}]	1.571
μ [mm^{-1}]	3.723
F(000)	1476
Crystal size [mm^3]	0.270×0.030×0.010
Crystal colour	purple
Crystal shape	block
Radiation	MoK_α (λ=0.71073 Å)
2θ range [°]	4.37 to 61.08 (0.70 Å)
Index ranges	−23 ≤ h ≤ 23
	−14 ≤ k ≤ 14
	−26 ≤ l ≤ 26
Reflections collected	72952
Independent reflections	9543
	R_{int} = 0.0753
	R_{sigma} = 0.0459
Completeness to θ = 25.242°	100.0 %
Data / Restraints / Parameters	9543/30/383
Absorption correction	0.6029/0.7461
T_{min}/T_{max} (method)	multi-scan
Goodness-of-fit on F^2	1.040
Final *R* indexes	R_1 = 0.0293
[$I \geq 2\sigma(I)$]	wR_2 = 0.0507
Final *R* indexes	R_1 = 0.0506
[all data]	wR_2 = 0.0582
Largest peak/hole [eÅ^{-3}]	1.41/−0.88

Table S3. Bond lengths and angles for **3**.

Atom–Atom	Length [Å]
Ta1–N4	1.794(7)
Ta1–N4A	1.815(13)
Ta1–N3	2.153(2)
Ta1–N1	2.158(2)
Ta1–N2	2.218(2)
Ta1–Cl2	2.4283(7)
Ta1–Cl1	2.4343(8)
N1–C2	1.346(3)
N1–C18	1.496(4)
N2–C1	1.323(4)
N2–C13	1.338(4)
N3–C12	1.353(3)
N3–C21	1.489(4)
C1–C6	1.427(4)
C1–C2	1.451(4)
C2–C3	1.431(4)
C3–C4	1.369(4)
C4–C5	1.436(4)
C4–C14	1.509(4)
C5–C6	1.360(4)
C6–C7	1.533(4)
C7–C8	1.528(4)
C7–C16	1.532(4)
C7–C15	1.555(4)
C8–C9	1.370(4)
C8–C13	1.420(4)
C9–C10	1.434(5)
C10–C11	1.370(4)
C10–C17	1.508(4)
C11–C12	1.428(4)
C12–C13	1.439(4)
C18–C20	1.517(4)
C18–C19	1.527(4)
C21–C23	1.509(5)
C21–C22	1.525(5)
N4–C24	1.380(7)
C24–C25	1.398(7)
C24–C29	1.400(7)
C25–C26	1.373(7)
C26–C27	1.378(9)
C27–C28	1.372(9)
C28–C29	1.404(8)
N4A–C24A	1.384(12)
C24A–C29A	1.394(11)
C24A–C25A	1.401(11)
C25A–C26A	1.393(12)
C26A–C27A	1.375(15)
C27A–C28A	1.388(13)
C28A–C29A	1.380(11)
C30–C31	1.495(17)
C31–C32	1.361(10)
C31–C36	1.368(10)
C32–C33	1.389(10)
C33–C34	1.415(10)
C34–C35	1.394(10)
C35–C36	1.394(10)

Atom–Atom–Atom	Angle [°]
N4–Ta1–N3	107.4(3)
N4A–Ta1–N3	111.5(6)
N4–Ta1–N1	106.6(4)
N4A–Ta1–N1	102.6(7)
N3–Ta1–N1	145.74(9)
N4–Ta1–N2	179.2(6)
N4A–Ta1–N2	175.5(6)
N3–Ta1–N2	73.09(9)
N1–Ta1–N2	72.85(9)
N4–Ta1–Cl2	96.7(6)
N4A–Ta1–Cl2	97.6(11)
N3–Ta1–Cl2	85.13(7)
N1–Ta1–Cl2	87.05(7)
N2–Ta1–Cl2	82.62(6)
N4–Ta1–Cl1	98.9(6)
N4A–Ta1–Cl1	98.1(11)
N3–Ta1–Cl1	88.92(7)
N1–Ta1–Cl1	89.76(7)
N2–Ta1–Cl1	81.76(6)
Cl2–Ta1–Cl1	164.30(2)
C2–N1–C18	118.7(2)
C2–N1–Ta1	118.00(19)
C18–N1–Ta1	123.22(18)
C1–N2–C13	124.2(2)
C1–N2–Ta1	118.07(18)
C13–N2–Ta1	117.46(19)
C12–N3–C21	117.9(2)
C12–N3–Ta1	117.2(2)
C21–N3–Ta1	124.11(18)
N2–C1–C6	121.6(3)
N2–C1–C2	114.3(2)
C6–C1–C2	124.0(3)
N1–C2–C3	128.3(3)
N1–C2–C1	116.6(3)
C3–C2–C1	115.1(2)
C4–C3–C2	121.1(3)
C3–C4–C5	121.2(3)
C3–C4–C14	120.5(3)
C5–C4–C14	118.4(3)
C6–C5–C4	121.6(3)
C5–C6–C1	116.9(3)
C5–C6–C7	124.6(3)
C1–C6–C7	118.2(3)
C8–C7–C16	112.2(3)
C8–C7–C6	112.0(2)
C16–C7–C6	111.5(3)
C8–C7–C15	106.1(2)
C16–C7–C15	108.7(2)
C6–C7–C15	105.9(2)
C9–C8–C13	116.5(3)
C9–C8–C7	125.4(3)
C13–C8–C7	117.9(3)
C8–C9–C10	121.4(3)
C11–C10–C9	121.3(3)
C11–C10–C17	120.5(3)
C9–C10–C17	118.2(3)
C10–C11–C12	120.6(3)
N3–C12–C11	127.5(3)
N3–C12–C13	116.8(3)
C11–C12–C13	115.7(3)
N2–C13–C8	121.5(3)
N2–C13–C12	114.2(2)
C8–C13–C12	124.2(3)
N1–C18–C20	110.6(2)
N1–C18–C19	110.5(2)
C20–C18–C19	112.1(2)
N3–C21–C23	110.4(3)
N3–C21–C22	110.2(3)
C23–C21–C22	112.2(3)
C24–N4–Ta1	173.6(10)
N4–C24–C25	119.9(9)
N4–C24–C29	121.6(9)
C25–C24–C29	118.5(5)

C26–C25–C24	120.9(5)	C26A–C27A–C28A	121.2(9)
C25–C26–C27	119.9(6)	C29A–C28A–C27A	120.3(10)
C28–C27–C26	121.3(5)	C28A–C29A–C24A	119.6(9)
C27–C28–C29	119.2(6)	C32–C31–C36	116.2(10)
C24–C29–C28	120.2(5)	C32–C31–C30	116.8(11)
C24A–N4A–Ta1	171(3)	C36–C31–C30	126.9(10)
N4A–C24A–C29A	119.4(17)	C31–C32–C33	123.6(12)
N4A–C24A–C25A	121.2(17)	C32–C33–C34	118.0(10)
C29A–C24A–C25A	119.4(9)	C35–C34–C33	120.3(10)
C26A–C25A–C24A	120.6(10)	C34–C35–C36	116.8(11)
C27A–C26A–C25A	118.7(11)	C31–C36–C35	125.0(11)

Bonds to hydrogen atoms were omitted.

Table S4. Torsion angles for **3**.

Atom–Atom–Atom–Atom	Torsion Angle [°]		
C13–N2–C1–C6	5.4(4)	C10–C11–C12–N3	−180.0(3)
Ta1–N2–C1–C6	178.9(2)	C10–C11–C12–C13	−1.1(4)
C13–N2–C1–C2	−171.7(2)	C1–N2–C13–C8	−2.0(4)
Ta1–N2–C1–C2	1.7(3)	Ta1–N2–C13–C8	−175.4(2)
C18–N1–C2–C3	−5.2(4)	C1–N2–C13–C12	174.1(3)
Ta1–N1–C2–C3	177.2(2)	Ta1–N2–C13–C12	0.7(3)
C18–N1–C2–C1	173.3(2)	C9–C8–C13–N2	170.8(3)
Ta1–N1–C2–C1	−4.3(3)	C7–C8–C13–N2	−14.2(4)
N2–C1–C2–N1	1.6(4)	C9–C8–C13–C12	−4.8(4)
C6–C1–C2–N1	−175.4(3)	C7–C8–C13–C12	170.2(3)
N2–C1–C2–C3	−179.7(2)	N3–C12–C13–N2	7.9(4)
C6–C1–C2–C3	3.3(4)	C11–C12–C13–N2	−171.1(2)
N1–C2–C3–C4	176.0(3)	N3–C12–C13–C8	−176.2(3)
C1–C2–C3–C4	−2.6(4)	C11–C12–C13–C8	4.8(4)
C2–C3–C4–C5	0.2(4)	C2–N1–C18–C20	−119.7(3)
C2–C3–C4–C14	179.7(3)	Ta1–N1–C18–C20	57.8(3)
C3–C4–C5–C6	1.9(4)	C2–N1–C18–C19	115.6(3)
C14–C4–C5–C6	−177.7(3)	Ta1–N1–C18–C19	−66.9(3)
C4–C5–C6–C1	−1.2(4)	C12–N3–C21–C23	93.2(3)
C4–C5–C6–C7	172.6(3)	Ta1–N3–C21–C23	−76.4(3)
N2–C1–C6–C5	−178.3(3)	C12–N3–C21–C22	−142.3(3)
C2–C1–C6–C5	−1.4(4)	Ta1–N3–C21–C22	48.1(3)
N2–C1–C6–C7	7.5(4)	N4–C24–C25–C26	−179.1(7)
C2–C1–C6–C7	−175.6(2)	C29–C24–C25–C26	−0.5(13)
C5–C6–C7–C8	165.0(3)	C24–C25–C26–C27	1.5(10)
C1–C6–C7–C8	−21.3(3)	C25–C26–C27–C28	−1.0(9)
C5–C6–C7–C16	38.3(4)	C26–C27–C28–C29	−0.6(10)
C1–C6–C7–C16	−148.0(3)	N4–C24–C29–C28	177.5(7)
C5–C6–C7–C15	−79.8(3)	C25–C24–C29–C28	−1.1(13)
C1–C6–C7–C15	94.0(3)	C27–C28–C29–C24	1.6(11)
C16–C7–C8–C9	−34.8(4)	N4A–C24A–C25A–C26A	−175.6(14)
C6–C7–C8–C9	−161.1(3)	C29A–C24A–C25A–C26A	3(2)
C15–C7–C8–C9	83.8(3)	C24A–C25A–C26A–C27A	−4(2)
C16–C7–C8–C13	150.7(3)	C25A–C26A–C27A–C28A	3(2)
C6–C7–C8–C13	24.4(4)	C26A–C27A–C28A–C29A	−1.2(19)
C15–C7–C8–C13	−90.7(3)	C27A–C28A–C29A–C24A	0(2)
C13–C8–C9–C10	1.1(4)	N4A–C24A–C29A–C28A	177.8(13)
C7–C8–C9–C10	−173.5(3)	C25A–C24A–C29A–C28A	−1(2)
C8–C9–C10–C11	2.4(5)	C36–C31–C32–C33	−3.1(15)
C8–C9–C10–C17	−179.3(3)	C30–C31–C32–C33	175.0(11)
C9–C10–C11–C12	−2.3(5)	C31–C32–C33–C34	4.0(16)
C17–C10–C11–C12	179.4(3)	C32–C33–C34–C35	−2.0(16)
C21–N3–C12–C11	−4.4(4)	C33–C34–C35–C36	−0.6(15)
Ta1–N3–C12–C11	165.9(2)	C32–C31–C36–C35	0.1(17)
C21–N3–C12–C13	176.8(3)	C30–C31–C36–C35	−177.7(13)
Ta1–N3–C12–C13	−12.9(3)	C34–C35–C36–C31	1.6(16)

Bonds to hydrogen atoms were omitted.

Crystallographic details of 4

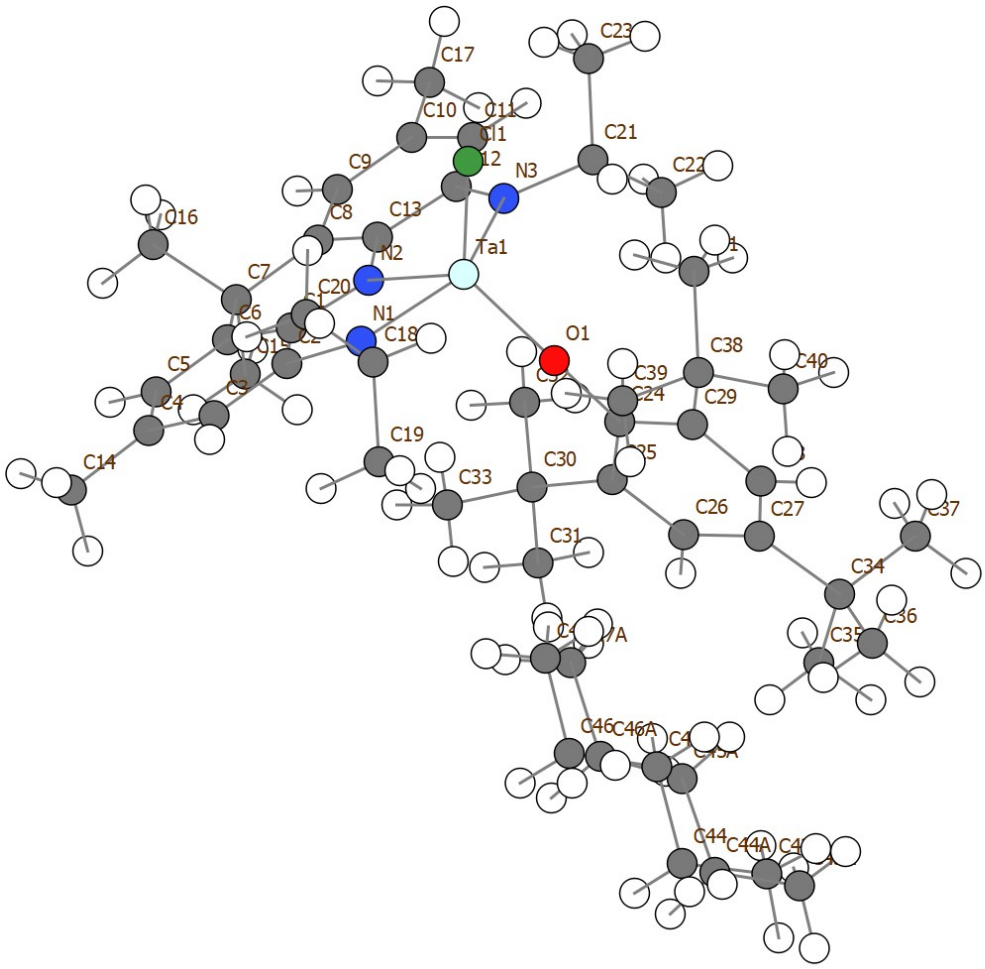

A red, plate-shaped crystal was mounted on a MiTeGen micromount with perfluoroether oil. Data for mo_ja24_sp_ii_93_3_0m_a were collected from a shock-cooled single crystal at 100(2) K on a Bruker D8 VENTURE dual wavelength Mo/Cu three-circle diffractometer with a microfocus sealed X-ray tube using a mirror optics as monochromator and a Bruker PHOTON III detector. The diffractometer was equipped with an Oxford Cryostream 800 low temperature device and used MoK_α radiation (λ = 0.71073 Å). All data were integrated with [No _computing_data_reduction given] and a multi-scan absorption correction using SADABS 2016/2 was applied.[1,2] The structure was solved by direct methods with SHELXT and refined by full-matrix least-squares methods against F^2 using SHELXL-2019/2.[3,4] All non-hydrogen atoms were refined with anisotropic displacement parameters. All hydrogen atoms were refined isotropic on calculated positions using a riding model with their U_{iso} values constrained to 1.5 times the U_{eq} of their pivot atoms for terminal sp^3 carbon atoms and 1.2 times for all other carbon atoms. Crystallographic data for the structures reported in this paper have been deposited with the Cambridge Crystallographic Data Centre.[5] CCDC 2402128 contain the supplementary crystallographic data for this paper. These data can be obtained free of charge from The Cambridge Crystallographic Data Centre via www.ccdc.cam.ac.uk/structures. This report and the CIF file were generated using FinalCif.[6]

Table S5. Crystal data and structure refinement for mo_ja24_sp_ii_93_3_0m_a (**4**).

CCDC number	2402128
Empirical formula	$C_{46}H_{71}ClN_3OTa$
Formula weight	898.45
Temperature [K]	100(2)
Crystal system	monoclinic
Space group (number)	$P2_1/c$ (14)
a [Å]	14.7961(3)
b [Å]	17.6077(4)
c [Å]	17.5721(3)
α [°]	90
β [°]	108.6340(10)
γ [°]	90
Volume [Å^3]	4337.99(15)
Z	4
ρ_{calc} [gcm^{-3}]	1.376
μ [mm^{-1}]	2.632
F(000)	1864
Crystal size [mm^3]	0.030×0.110×0.130
Crystal colour	red
Crystal shape	plate
Radiation	MoK_α (λ=0.71073 Å)
2θ range [°]	4.63 to 50.81 (0.83 Å)
Index ranges	−17 ≤ h ≤ 17
	−21 ≤ k ≤ 21
	−20 ≤ l ≤ 21
Reflections collected	132145
Independent reflections	7961
	R_{int} = 0.0608
	R_{sigma} = 0.0207
Completeness to θ = 25.242°	99.9 %
Data / Restraints / Parameters	7961 / 0 / 470
Absorption correction T_{min}/T_{max} (method)	0.6419 / 0.7452 (multi-scan)
Goodness-of-fit on F^2	0.979
Final *R* indexes	R_1 = 0.0190
[$I \geq 2\sigma(I)$]	wR_2 = 0.0434
Final *R* indexes	R_1 = 0.0219
[all data]	wR_2 = 0.0456
Largest peak/hole [eÅ^{-3}]	0.75/−0.48

Table S6. Bond lengths and angles for **4**.

Atom–Atom	Length [Å]
Ta1–O1	1.8984(15)
Ta1–N1	2.0080(19)
Ta1–N3	2.0138(19)
Ta1–N2	2.0316(19)
Ta1–Cl1	2.3349(6)
O1–C24	1.388(3)
N1–C2	1.400(3)
N1–C18	1.478(3)
N2–C13	1.390(3)
N2–C1	1.394(3)
N3–C12	1.400(3)
N3–C21	1.483(3)
C1–C6	1.386(3)
C1–C2	1.400(3)
C2–C3	1.391(3)
C3–C4	1.397(3)
C4–C5	1.395(3)
C4–C14	1.513(3)
C5–C6	1.397(3)
C6–C7	1.541(3)
C7–C8	1.530(3)
C7–C16	1.536(3)
C7–C15	1.540(3)
C8–C13	1.384(3)
C8–C9	1.398(3)
C9–C10	1.392(3)
C10–C11	1.402(3)
C10–C17	1.509(3)
C11–C12	1.391(3)
C12–C13	1.406(3)
C18–C19	1.530(3)
C18–C20	1.531(3)
C21–C22	1.525(3)
C21–C23	1.529(3)
C24–C25	1.415(3)
C24–C29	1.420(3)
C25–C26	1.400(3)
C25–C30	1.542(3)
C26–C27	1.387(3)
C27–C28	1.390(3)
C27–C34	1.541(3)
C28–C29	1.397(3)
C29–C38	1.544(3)
C30–C31	1.537(3)
C30–C32	1.537(3)
C30–C33	1.538(3)
C34–C36	1.528(4)
C34–C35	1.530(4)
C34–C37	1.536(4)
C38–C39	1.538(3)
C38–C40	1.539(3)
C38–C41	1.540(3)
C43–C44	1.513(8)
C44–C45	1.515(7)
C45–C46	1.557(7)
C46–C47	1.506(7)
C43A–C44A	1.487(15)
C44A–C45A	1.517(14)
C45A–C46A	1.557(14)
C46A–C47A	1.508(14)

Atom–Atom–Atom	Angle [°]
O1–Ta1–N1	101.48(7)
O1–Ta1–N3	101.77(7)
N1–Ta1–N3	144.86(8)
O1–Ta1–N2	121.55(7)
N1–Ta1–N2	72.63(7)
N3–Ta1–N2	72.81(7)
O1–Ta1–Cl1	116.40(5)
N1–Ta1–Cl1	97.58(6)
N3–Ta1–Cl1	95.25(6)
N2–Ta1–Cl1	122.04(6)
C24–O1–Ta1	166.46(15)
C2–N1–C18	123.40(19)
C2–N1–Ta1	123.70(15)
C18–N1–Ta1	112.90(14)
C13–N2–C1	116.33(19)
C13–N2–Ta1	121.96(15)
C1–N2–Ta1	121.71(15)
C12–N3–C21	122.42(19)
C12–N3–Ta1	123.40(15)
C21–N3–Ta1	114.14(15)
C6–C1–N2	125.1(2)
C6–C1–C2	123.0(2)
N2–C1–C2	111.9(2)
C3–C2–N1	131.1(2)
C3–C2–C1	119.2(2)
N1–C2–C1	109.66(19)
C2–C3–C4	119.2(2)
C5–C4–C3	120.0(2)
C5–C4–C14	120.3(2)
C3–C4–C14	119.7(2)
C4–C5–C6	122.0(2)
C1–C6–C5	116.5(2)
C1–C6–C7	121.1(2)
C5–C6–C7	122.3(2)
C8–C7–C16	109.89(19)
C8–C7–C15	108.64(19)
C16–C7–C15	109.4(2)
C8–C7–C6	110.49(19)
C16–C7–C6	109.67(18)
C15–C7–C6	108.73(19)
C13–C8–C9	116.7(2)
C13–C8–C7	121.5(2)
C9–C8–C7	121.8(2)
C10–C9–C8	121.9(2)
C9–C10–C11	120.2(2)
C9–C10–C17	120.7(2)
C11–C10–C17	119.1(2)
C12–C11–C10	119.1(2)
C11–C12–N3	131.1(2)
C11–C12–C13	119.0(2)
N3–C12–C13	109.9(2)
C8–C13–N2	125.1(2)
C8–C13–C12	123.0(2)
N2–C13–C12	111.9(2)
N1–C18–C19	113.57(19)
N1–C18–C20	111.09(19)
C19–C18–C20	114.1(2)
N3–C21–C22	113.1(2)
N3–C21–C23	111.80(19)
C22–C21–C23	114.1(2)
O1–C24–C25	120.9(2)
O1–C24–C29	117.8(2)
C25–C24–C29	121.3(2)
C26–C25–C24	117.0(2)
C26–C25–C30	118.4(2)
C24–C25–C30	124.7(2)
C27–C26–C25	123.7(2)
C26–C27–C28	117.2(2)
C26–C27–C34	122.3(2)

C28–C27–C34	120.5(2)	C35–C34–C27	112.4(2)
C27–C28–C29	123.2(2)	C37–C34–C27	109.2(2)
C28–C29–C24	117.3(2)	C39–C38–C40	106.62(19)
C28–C29–C38	119.3(2)	C39–C38–C41	110.7(2)
C24–C29–C38	123.4(2)	C40–C38–C41	106.1(2)
C31–C30–C32	106.0(2)	C39–C38–C29	109.26(19)
C31–C30–C33	105.8(2)	C40–C38–C29	112.35(19)
C32–C30–C33	112.1(2)	C41–C38–C29	111.65(19)
C31–C30–C25	112.61(19)	C43–C44–C45	113.9(5)
C32–C30–C25	109.70(19)	C44–C45–C46	114.6(4)
C33–C30–C25	110.5(2)	C47–C46–C45	112.9(4)
C36–C34–C35	108.0(2)	C43A–C44A–C45A	111.0(12)
C36–C34–C37	108.5(2)	C44A–C45A–C46A	113.3(10)
C35–C34–C37	108.3(2)	C47A–C46A–C45A	111.4(11)
C36–C34–C27	110.4(2)		

Table S7. Torsion angles for **4**.

Atom–Atom–Atom–Atom	Torsion Angle [°]		
N1–Ta1–O1–C24	112.3(6)	Ta1–N3–C12–C11	179.21(19)
N3–Ta1–O1–C24	−41.2(6)	C21–N3–C12–C13	176.2(2)
N2–Ta1–O1–C24	35.8(6)	Ta1–N3–C12–C13	−1.4(3)
Cl1–Ta1–O1–C24	−143.1(6)	C9–C8–C13–N2	177.6(2)
C13–N2–C1–C6	4.0(3)	C7–C8–C13–N2	−3.4(3)
Ta1–N2–C1–C6	−175.04(17)	C9–C8–C13–C12	−2.2(3)
C13–N2–C1–C2	−175.86(19)	C7–C8–C13–C12	176.8(2)
Ta1–N2–C1–C2	5.1(3)	C1–N2–C13–C8	−2.2(3)
C18–N1–C2–C3	−6.8(4)	Ta1–N2–C13–C8	176.81(17)
Ta1–N1–C2–C3	173.91(19)	C1–N2–C13–C12	177.57(19)
C18–N1–C2–C1	175.2(2)	Ta1–N2–C13–C12	−3.4(3)
Ta1–N1–C2–C1	−4.1(3)	C11–C12–C13–C8	2.1(3)
C6–C1–C2–C3	1.2(3)	N3–C12–C13–C8	−177.4(2)
N2–C1–C2–C3	−178.9(2)	C11–C12–C13–N2	−177.7(2)
C6–C1–C2–N1	179.5(2)	N3–C12–C13–N2	2.8(3)
N2–C1–C2–N1	−0.7(3)	C2–N1–C18–C19	65.3(3)
N1–C2–C3–C4	−177.5(2)	Ta1–N1–C18–C19	−115.34(19)
C1–C2–C3–C4	0.3(3)	C2–N1–C18–C20	−65.0(3)
C2–C3–C4–C5	−1.5(3)	Ta1–N1–C18–C20	114.42(18)
C2–C3–C4–C14	177.2(2)	C12–N3–C21–C22	−63.1(3)
C3–C4–C5–C6	1.1(3)	Ta1–N3–C21–C22	114.60(19)
C14–C4–C5–C6	−177.5(2)	C12–N3–C21–C23	67.4(3)
N2–C1–C6–C5	178.7(2)	Ta1–N3–C21–C23	−114.92(19)
C2–C1–C6–C5	−1.5(3)	Ta1–O1–C24–C25	−34.7(7)
N2–C1–C6–C7	−0.1(3)	Ta1–O1–C24–C29	145.7(5)
C2–C1–C6–C7	179.7(2)	O1–C24–C25–C26	174.6(2)
C4–C5–C6–C1	0.3(3)	C29–C24–C25–C26	−5.8(3)
C4–C5–C6–C7	179.1(2)	O1–C24–C25–C30	−5.2(3)
C1–C6–C7–C8	−4.9(3)	C29–C24–C25–C30	174.4(2)
C5–C6–C7–C8	176.4(2)	C24–C25–C26–C27	1.2(4)
C1–C6–C7–C16	−126.2(2)	C30–C25–C26–C27	−179.1(2)
C5–C6–C7–C16	55.1(3)	C25–C26–C27–C28	2.7(4)
C1–C6–C7–C15	114.2(2)	C25–C26–C27–C34	−177.0(2)
C5–C6–C7–C15	−64.5(3)	C26–C27–C28–C29	−2.0(4)
C16–C7–C8–C13	127.7(2)	C34–C27–C28–C29	177.7(2)
C15–C7–C8–C13	−112.7(2)	C27–C28–C29–C24	−2.4(4)
C6–C7–C8–C13	6.6(3)	C27–C28–C29–C38	175.6(2)
C16–C7–C8–C9	−53.3(3)	O1–C24–C29–C28	−173.9(2)
C15–C7–C8–C9	66.3(3)	C25–C24–C29–C28	6.4(3)
C6–C7–C8–C9	−174.5(2)	O1–C24–C29–C38	8.1(3)
C13–C8–C9–C10	0.2(3)	C25–C24–C29–C38	−171.5(2)
C7–C8–C9–C10	−178.9(2)	C26–C25–C30–C31	7.0(3)
C8–C9–C10–C11	1.9(4)	C24–C25–C30–C31	−173.3(2)
C8–C9–C10–C17	−178.7(2)	C26–C25–C30–C32	−110.8(2)
C9–C10–C11–C12	−2.0(3)	C24–C25–C30–C32	69.0(3)
C17–C10–C11–C12	178.6(2)	C26–C25–C30–C33	125.1(2)
C10–C11–C12–N3	179.4(2)	C24–C25–C30–C33	−55.2(3)
C10–C11–C12–C13	0.0(3)	C26–C27–C34–C36	−132.7(3)
C21–N3–C12–C11	−3.3(4)	C28–C27–C34–C36	47.6(3)
		C26–C27–C34–C35	−12.1(3)

C28–C27–C34–C35	168.2(2)	C28–C29–C38–C41	120.2(2)
C26–C27–C34–C37	108.1(3)	C24–C29–C38–C41	−61.9(3)
C28–C27–C34–C37	−71.6(3)	C43–C44–C45–C46	177.9(5)
C28–C29–C38–C39	−117.0(2)	C44–C45–C46–C47	179.2(5)
C24–C29–C38–C39	60.9(3)	C43A–C44A–C45A–C46A	−172.1(13)
C28–C29–C38–C40	1.1(3)		
C24–C29–C38–C40	179.0(2)		

Crystallographic Details of 5

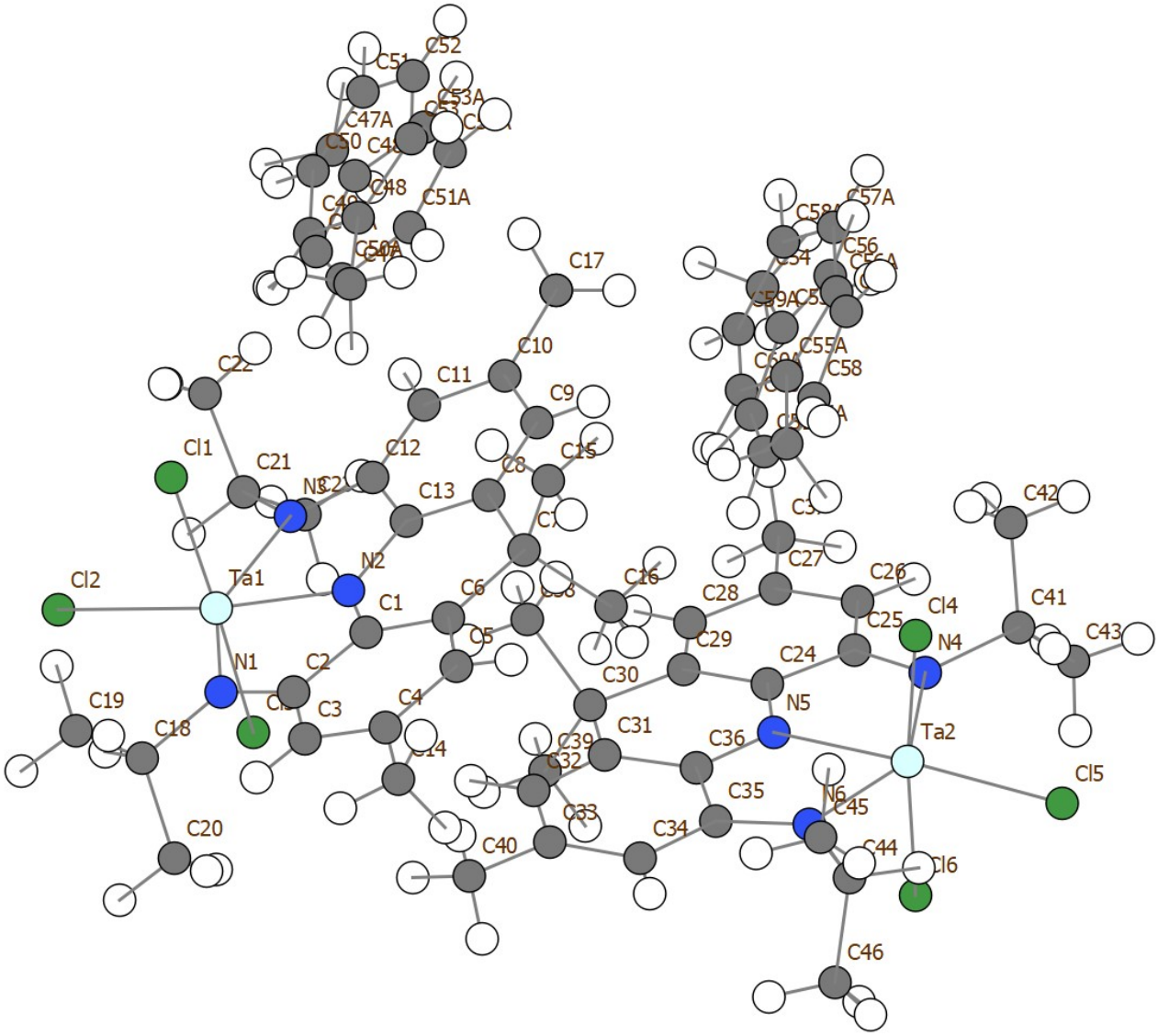

A green, block-shaped crystal of mo_ja24_sp_iii_01_0ma_a (**5**) was mounted on a MiTeGen micromount with perfluoroether oil. Data were collected from a shock-cooled single crystal at 102(2) K on a Bruker D8 VENTURE dual wavelength Mo/Cu three-circle diffractometer with a microfocus sealed X-ray tube using a mirror optics as monochromator and a Bruker PHOTON III detector. The diffractometer was equipped with an Oxford Cryostream 800 low temperature device and used MoK_α radiation (λ = 0.71073 Å). All data were integrated with SAINT and a multi-scan absorption correction using SADABS was applied.[12,13] The structure was solved by direct methods using SHELXT and refined by full-matrix least-squares methods against F^2 by SHELXL-2019/2.[15,15] All non-hydrogen atoms were refined with anisotropic displacement parameters. All C-bound hydrogen atoms were refined isotropic on calculated positions using a riding model with their U_{iso} values constrained to 1.5 times the U_{eq} of their pivot atoms for terminal sp^3 carbon atoms and 1.2 times for all other carbon atoms. Disordered moieties were refined using bond lengths restraints and displacement parameter restraints. Crystallographic data for the structures reported here have been deposited with the Cambridge Crystallographic Data Centre.[16] CCDC 2383360 contain the supplementary crystallographic data for this paper. These data can be obtained free of charge from The Cambridge Crystallographic Data Centre via www.ccdc.cam.ac.uk/structures. This report and the CIF file were generated using FinalCif.[17]

Table S7. Crystal data and structure refinement for mo_ja24_sp_iii_01_0ma_a (**5**).

CCDC number	2383360
Empirical formula	$C_{30}H_{38}Cl_3N_3Ta$
Formula weight	727.93
Temperature [K]	102(2)
Crystal system	monoclinic
Space group (number)	$P2_1/c$ (14)
a [Å]	21.2427(5)
b [Å]	17.3990(5)
c [Å]	16.6559(4)
α [°]	90
β [°]	100.4230(10)
γ [°]	90
Volume [Å^3]	6054.5(3)
Z	8
ρ_{calc} [gcm^{-3}]	1.597
μ [mm^{-1}]	3.919
F(000)	2904
Crystal size [mm^3]	0.150×0.060×0.060
Crystal colour	green
Crystal shape	block
Radiation	MoK_α (λ=0.71073 Å)
2θ range [°]	3.90 to 56.67 (0.75 Å)
Index ranges	−27 ≤ h ≤ 28
	−23 ≤ k ≤ 23
	−22 ≤ l ≤ 22
Reflections collected	109358
Independent reflections	15075
	R_{int} = 0.0900
	R_{sigma} = 0.0519
Completeness to θ = 25.242°	100.0 %
Data / Restraints / Parameters	15075/90/665
Absorption correction	0.6123/0.7457
T_{min}/T_{max} (method)	multi-scan
Goodness-of-fit on F^2	1.015
Final *R* indexes	R_1 = 0.0372
[$I \geq 2\sigma(I)$]	wR_2 = 0.0756
Final *R* indexes	R_1 = 0.0540
[all data]	wR_2 = 0.0842
Largest peak/hole [eÅ^{-3}]	1.83/−1.47

Table S8. Bond lengths and angles for **5**.

Atom–Atom	Length [Å]
Ta1–N3	2.025(4)
Ta1–N1	2.028(4)
Ta1–N2	2.136(3)
Ta1–Cl2	2.3747(12)
Ta1–Cl3	2.3767(12)
Ta1–Cl1	2.4284(12)
Ta2–N6	2.033(3)
Ta2–N4	2.036(3)
Ta2–N5	2.142(3)
Ta2–Cl4	2.3747(12)
Ta2–Cl5	2.3961(12)
Ta2–Cl6	2.4079(11)
N1–C2	1.371(5)
N1–C18	1.491(5)
N2–C1	1.361(5)
N2–C13	1.362(5)
N3–C12	1.373(6)
N3–C21	1.490(5)
N4–C25	1.380(5)
N4–C41	1.493(6)
N5–C24	1.354(5)
N5–C36	1.354(5)
N6–C35	1.374(6)
N6–C44	1.481(6)
C1–C2	1.408(6)
C1–C6	1.411(6)
C2–C3	1.417(6)
C3–C4	1.384(6)
C4–C5	1.414(6)
C4–C14	1.499(6)
C5–C6	1.385(6)
C6–C7	1.528(6)
C7–C15	1.534(6)
C7–C8	1.540(6)
C7–C16	1.546(6)
C8–C9	1.381(6)
C8–C13	1.398(6)
C9–C10	1.417(6)
C10–C11	1.390(7)
C10–C17	1.505(6)
C11–C12	1.398(6)
C12–C13	1.422(6)
C18–C20	1.516(7)
C18–C19	1.526(7)
C21–C23	1.521(6)
C21–C22	1.522(6)
C24–C29	1.411(6)
C24–C25	1.413(6)
C25–C26	1.390(6)
C26–C27	1.394(7)
C27–C28	1.405(6)
C27–C37	1.512(6)
C28–C29	1.385(6)
C29–C30	1.533(6)
C30–C31	1.528(6)
C30–C38	1.536(6)
C30–C39	1.539(6)
C31–C32	1.376(6)
C31–C36	1.411(6)
C32–C33	1.410(6)
C33–C34	1.385(6)
C33–C40	1.507(6)
C34–C35	1.408(6)
C35–C36	1.423(6)
C41–C42	1.508(7)
C41–C43	1.510(7)
C44–C45	1.513(7)
C44–C46	1.523(7)
C47–C48	1.506(11)
C48–C49	1.371(11)
C48–C53	1.375(10)
C49–C50	1.396(12)
C50–C51	1.351(11)
C51–C52	1.375(11)
C52–C53	1.374(11)
C47A–C48A	1.523(16)
C48A–C53A	1.379(15)
C48A–C49A	1.385(15)
C49A–C50A	1.388(18)
C50A–C51A	1.372(16)
C51A–C52A	1.400(16)
C52A–C53A	1.354(16)
C54–C55	1.481(14)
C55–C60	1.380(12)
C55–C56	1.401(13)
C56–C57	1.378(17)
C57–C58	1.369(13)
C58–C59	1.439(13)
C59–C60	1.326(14)
C54A–C55A	1.498(15)
C55A–C60A	1.379(14)
C55A–C56A	1.394(14)
C56A–C57A	1.375(18)
C57A–C58A	1.360(15)
C58A–C59A	1.432(15)
C59A–C60A	1.321(15)

Atom–Atom–Atom	Angle [°]
N3–Ta1–N1	143.73(14)
N3–Ta1–N2	71.77(14)
N1–Ta1–N2	71.98(14)
N3–Ta1–Cl2	109.70(11)
N1–Ta1–Cl2	106.17(11)
N2–Ta1–Cl2	169.62(10)
N3–Ta1–Cl3	91.95(11)
N1–Ta1–Cl3	92.44(11)
N2–Ta1–Cl3	98.91(10)
Cl2–Ta1–Cl3	91.35(5)
N3–Ta1–Cl1	86.95(11)
N1–Ta1–Cl1	90.38(11)
N2–Ta1–Cl1	83.86(10)
Cl2–Ta1–Cl1	85.95(5)
Cl3–Ta1–Cl1	176.55(4)
N6–Ta2–N4	143.53(14)
N6–Ta2–N5	71.80(14)
N4–Ta2–N5	71.89(14)
N6–Ta2–Cl4	90.47(11)
N4–Ta2–Cl4	92.06(11)
N5–Ta2–Cl4	99.38(10)
N6–Ta2–Cl5	112.55(11)
N4–Ta2–Cl5	103.88(11)
N5–Ta2–Cl5	170.99(10)
Cl4–Ta2–Cl5	88.62(4)
N6–Ta2–Cl6	90.21(11)
N4–Ta2–Cl6	91.61(11)
N5–Ta2–Cl6	87.58(10)
Cl4–Ta2–Cl6	172.86(4)
Cl5–Ta2–Cl6	84.56(4)
C2–N1–C18	122.3(4)
C2–N1–Ta1	123.3(3)
C18–N1–Ta1	114.3(3)

C1–N2–C13	119.3(4)	C28–C27–C37	119.6(4)
C1–N2–Ta1	119.5(3)	C29–C28–C27	121.8(4)
C13–N2–Ta1	119.7(3)	C28–C29–C24	115.8(4)
C12–N3–C21	123.2(4)	C28–C29–C30	123.2(4)
C12–N3–Ta1	123.6(3)	C24–C29–C30	121.0(4)
C21–N3–Ta1	113.2(3)	C31–C30–C29	111.2(4)
C25–N4–C41	121.3(4)	C31–C30–C38	109.5(4)
C25–N4–Ta2	122.8(3)	C29–C30–C38	108.2(4)
C41–N4–Ta2	115.7(3)	C31–C30–C39	109.1(4)
C24–N5–C36	120.1(4)	C29–C30–C39	109.0(4)
C24–N5–Ta2	119.6(3)	C38–C30–C39	109.7(4)
C36–N5–Ta2	120.1(3)	C32–C31–C36	116.1(4)
C35–N6–C44	123.0(4)	C32–C31–C30	123.5(4)
C35–N6–Ta2	123.9(3)	C36–C31–C30	120.4(4)
C44–N6–Ta2	113.1(3)	C31–C32–C33	122.2(4)
N2–C1–C2	112.5(4)	C34–C33–C32	120.9(4)
N2–C1–C6	123.6(4)	C34–C33–C40	119.0(4)
C2–C1–C6	123.9(4)	C32–C33–C40	120.1(4)
N1–C2–C1	112.3(4)	C33–C34–C35	119.6(4)
N1–C2–C3	129.9(4)	N6–C35–C34	130.8(4)
C1–C2–C3	117.7(4)	N6–C35–C36	111.6(4)
C4–C3–C2	119.5(4)	C34–C35–C36	117.6(4)
C3–C4–C5	120.9(4)	N5–C36–C31	123.9(4)
C3–C4–C14	120.4(4)	N5–C36–C35	112.6(4)
C5–C4–C14	118.7(4)	C31–C36–C35	123.5(4)
C6–C5–C4	121.9(4)	N4–C41–C42	111.4(4)
C5–C6–C1	116.1(4)	N4–C41–C43	112.6(4)
C5–C6–C7	123.1(4)	C42–C41–C43	114.9(4)
C1–C6–C7	120.8(4)	N6–C44–C45	112.5(4)
C6–C7–C15	109.7(4)	N6–C44–C46	111.7(4)
C6–C7–C8	110.8(3)	C45–C44–C46	114.9(4)
C15–C7–C8	109.7(4)	C49–C48–C53	118.5(8)
C6–C7–C16	108.7(4)	C49–C48–C47	120.4(8)
C15–C7–C16	109.9(4)	C53–C48–C47	121.1(8)
C8–C7–C16	108.0(3)	C48–C49–C50	120.4(8)
C9–C8–C13	116.3(4)	C51–C50–C49	120.6(9)
C9–C8–C7	123.0(4)	C50–C51–C52	119.0(9)
C13–C8–C7	120.7(4)	C53–C52–C51	120.8(9)
C8–C9–C10	121.4(4)	C52–C53–C48	120.6(9)
C11–C10–C9	121.2(4)	C53A–C48A–C49A	118.2(14)
C11–C10–C17	119.8(4)	C53A–C48A–C47A	119.9(15)
C9–C10–C17	118.9(4)	C49A–C48A–C47A	121.4(15)
C10–C11–C12	119.2(4)	C48A–C49A–C50A	121.5(16)
N3–C12–C11	130.4(4)	C51A–C50A–C49A	118.9(16)
N3–C12–C13	111.7(4)	C50A–C51A–C52A	119.8(15)
C11–C12–C13	117.8(4)	C53A–C52A–C51A	120.2(16)
N2–C13–C8	124.0(4)	C52A–C53A–C48A	121.3(15)
N2–C13–C12	112.0(4)	C60–C55–C56	116.2(12)
C8–C13–C12	124.0(4)	C60–C55–C54	124.0(11)
N1–C18–C20	112.4(4)	C56–C55–C54	119.7(11)
N1–C18–C19	111.2(4)	C57–C56–C55	121.1(12)
C20–C18–C19	115.4(4)	C58–C57–C56	120.9(12)
N3–C21–C23	111.6(4)	C57–C58–C59	118.4(12)
N3–C21–C22	112.4(4)	C60–C59–C58	118.4(12)
C23–C21–C22	114.7(4)	C59–C60–C55	125.0(12)
N5–C24–C29	123.2(4)	C60A–C55A–C56A	117.5(14)
N5–C24–C25	112.8(4)	C60A–C55A–C54A	123.3(13)
C29–C24–C25	124.1(4)	C56A–C55A–C54A	119.2(14)
N4–C25–C26	130.4(4)	C57A–C56A–C55A	119.7(15)
N4–C25–C24	112.0(4)	C58A–C57A–C56A	122.2(14)
C26–C25–C24	117.6(4)	C57A–C58A–C59A	117.3(14)
C25–C26–C27	119.9(4)	C60A–C59A–C58A	119.8(14)
C26–C27–C28	120.8(4)	C59A–C60A–C55A	123.4(14)
C26–C27–C37	119.6(4)		

Bonds to hydrogen atoms were omitted.

Table S9. Torsion angles for **5.**

Atom–Atom–Atom–Atom	Torsion Angle [°]
C13–N2–C1–C2	170.9(4)
Ta1–N2–C1–C2	5.1(5)
C13–N2–C1–C6	−7.5(6)
Ta1–N2–C1–C6	−173.2(3)
C18–N1–C2–C1	171.2(4)
Ta1–N1–C2–C1	−5.0(5)
C18–N1–C2–C3	−10.1(7)
Ta1–N1–C2–C3	173.7(4)
N2–C1–C2–N1	−0.4(5)
C6–C1–C2–N1	178.0(4)
N2–C1–C2–C3	−179.2(4)
C6–C1–C2–C3	−0.9(6)
N1–C2–C3–C4	−179.7(4)
C1–C2–C3–C4	−1.1(6)
C2–C3–C4–C5	1.6(7)
C2–C3–C4–C14	−177.7(4)
C3–C4–C5–C6	−0.1(7)
C14–C4–C5–C6	179.2(4)
C4–C5–C6–C1	−1.8(7)
C4–C5–C6–C7	178.5(4)
N2–C1–C6–C5	−179.5(4)
C2–C1–C6–C5	2.3(6)
N2–C1–C6–C7	0.2(6)
C2–C1–C6–C7	−178.0(4)
C5–C6–C7–C15	−51.4(6)
C1–C6–C7–C15	128.9(4)
C5–C6–C7–C8	−172.6(4)
C1–C6–C7–C8	7.7(6)
C5–C6–C7–C16	68.9(5)
C1–C6–C7–C16	−110.8(4)
C6–C7–C8–C9	171.3(4)
C15–C7–C8–C9	50.0(6)
C16–C7–C8–C9	−69.8(5)
C6–C7–C8–C13	−9.3(6)
C15–C7–C8–C13	−130.5(4)
C16–C7–C8–C13	109.7(4)
C13–C8–C9–C10	−0.3(7)
C7–C8–C9–C10	179.2(4)
C8–C9–C10–C11	−2.3(7)
C8–C9–C10–C17	174.7(4)
C9–C10–C11–C12	2.7(7)
C17–C10–C11–C12	−174.2(4)
C21–N3–C12–C11	9.6(7)
Ta1–N3–C12–C11	−168.4(4)
C21–N3–C12–C13	−173.2(4)
Ta1–N3–C12–C13	8.7(5)
C10–C11–C12–N3	176.3(4)
C10–C11–C12–C13	−0.7(6)
C1–N2–C13–C8	5.7(6)
Ta1–N2–C13–C8	171.5(3)
C1–N2–C13–C12	−174.1(4)
Ta1–N2–C13–C12	−8.4(5)
C9–C8–C13–N2	−177.3(4)
C7–C8–C13–N2	3.2(6)
C9–C8–C13–C12	2.5(6)
C7–C8–C13–C12	−177.0(4)
N3–C12–C13–N2	0.3(5)
C11–C12–C13–N2	177.8(4)
N3–C12–C13–C8	−179.6(4)
C11–C12–C13–C8	−2.0(6)
C2–N1–C18–C20	−56.0(5)
Ta1–N1–C18–C20	120.5(4)
C2–N1–C18–C19	75.1(5)
Ta1–N1–C18–C19	−108.4(4)
C12–N3–C21–C23	59.9(6)
Ta1–N3–C21–C23	−121.9(4)
C12–N3–C21–C22	−70.6(5)
Ta1–N3–C21–C22	107.6(4)
C36–N5–C24–C29	−1.0(6)
Ta2–N5–C24–C29	174.1(3)
C36–N5–C24–C25	179.0(4)
Ta2–N5–C24–C25	−5.9(5)
C41–N4–C25–C26	14.7(7)
Ta2–N4–C25–C26	−170.2(4)
C41–N4–C25–C24	−166.6(4)
Ta2–N4–C25–C24	8.5(5)
N5–C24–C25–N4	−1.2(5)
C29–C24–C25–N4	178.8(4)
N5–C24–C25–C26	177.7(4)
C29–C24–C25–C26	−2.3(6)
N4–C25–C26–C27	178.8(4)
C24–C25–C26–C27	0.2(7)
C25–C26–C27–C28	1.3(7)
C25–C26–C27–C37	−179.6(4)
C26–C27–C28–C29	−0.8(7)
C37–C27–C28–C29	−179.8(5)
C27–C28–C29–C24	−1.2(7)
C27–C28–C29–C30	178.4(4)
N5–C24–C29–C28	−177.2(4)
C25–C24–C29–C28	2.8(6)
N5–C24–C29–C30	3.2(6)
C25–C24–C29–C30	−176.8(4)
C28–C29–C30–C31	179.1(4)
C24–C29–C30–C31	−1.3(6)
C28–C29–C30–C38	−60.6(6)
C24–C29–C30–C38	119.0(4)
C28–C29–C30–C39	58.7(6)
C24–C29–C30–C39	−121.7(4)
C29–C30–C31–C32	178.0(4)
C38–C30–C31–C32	58.5(6)
C39–C30–C31–C32	−61.7(5)
C29–C30–C31–C36	−2.5(6)
C38–C30–C31–C36	−122.0(4)
C39–C30–C31–C36	117.8(4)
C36–C31–C32–C33	−2.7(6)
C30–C31–C32–C33	176.8(4)
C31–C32–C33–C34	−0.5(7)
C31–C32–C33–C40	177.9(4)
C32–C33–C34–C35	2.3(7)
C40–C33–C34–C35	−176.1(4)
C44–N6–C35–C34	1.8(7)
Ta2–N6–C35–C34	−177.5(4)
C44–N6–C35–C36	−178.5(4)
Ta2–N6–C35–C36	2.3(5)
C33–C34–C35–N6	178.9(4)
C33–C34–C35–C36	−0.9(6)
C24–N5–C36–C31	−3.2(6)
Ta2–N5–C36–C31	−178.3(3)
C24–N5–C36–C35	177.1(4)
Ta2–N5–C36–C35	2.0(5)
C32–C31–C36–N5	−175.5(4)
C30–C31–C36–N5	5.0(6)
C32–C31–C36–C35	4.2(6)
C30–C31–C36–C35	−175.3(4)
N6–C35–C36–N5	−2.6(5)
C34–C35–C36–N5	177.2(4)
N6–C35–C36–C31	177.7(4)
C34–C35–C36–C31	−2.5(6)
C25–N4–C41–C42	57.2(6)
Ta2–N4–C41–C42	−118.2(4)
C25–N4–C41–C43	−73.5(5)

Ta2–N4–C41–C43	111.1(4)
C35–N6–C44–C45	−63.9(6)
Ta2–N6–C44–C45	115.4(4)
C35–N6–C44–C46	67.0(5)
Ta2–N6–C44–C46	−113.6(4)
C53–C48–C49–C50	−1.4(15)
C47–C48–C49–C50	175.5(10)
C48–C49–C50–C51	0.3(16)
C49–C50–C51–C52	0.5(14)
C50–C51–C52–C53	−0.2(14)
C51–C52–C53–C48	−0.9(14)
C49–C48–C53–C52	1.6(14)
C47–C48–C53–C52	−175.2(9)
C53A–C48A–C49A–C50A	3(4)
C47A–C48A–C49A–C50A	175(2)
C48A–C49A–C50A–C51A	0(4)
C49A–C50A–C51A–C52A	−1(3)
C50A–C51A–C52A–C53A	−1(3)
C51A–C52A–C53A–C48A	4(3)
C13–C8–C9–C10	−3.2(2)
C7–C8–C9–C10	177.39(13)
C8–C9–C10–C11	1.9(2)
C8–C9–C10–C17	−177.48(14)
C9–C10–C11–C12	1.3(2)
C17–C10–C11–C12	−179.23(14)
C10–C11–C12–N3	−179.01(14)
C10–C11–C12–C13	−3.2(2)
C21–N3–C12–C11	−4.7(2)
C21–N3–C12–C13	179.36(13)
C9–C8–C13–N2	−178.06(13)
C7–C8–C13–N2	1.3(2)
C9–C8–C13–C12	1.3(2)
C7–C8–C13–C12	−179.33(12)
C1–N2–C13–C8	−11.7(2)
C1–N2–C13–C12	168.89(12)
C11–C12–C13–C8	1.8(2)
N3–C12–C13–C8	177.90(13)
C11–C12–C13–N2	−178.77(13)
N3–C12–C13–N2	−2.68(19)
C2–N1–C18–C19	156.80(13)
C2–N1–C18–C20	−82.23(17)
C12–N3–C21–C23	166.78(14)
C12–N3–C21–C22	−70.04(18)
C18–N1–C2–C3	7.9(2)
C18–N1–C2–C1	−173.50(13)
C6–C1–C2–C3	−3.5(2)
N2–C1–C2–C3	179.05(13)
C6–C1–C2–N1	177.88(12)
N2–C1–C2–N1	0.40(19)
N1–C2–C3–C4	−179.76(14)
C1–C2–C3–C4	1.7(2)
C6–C5–C4–C3	−2.4(2)
C6–C5–C4–C14	178.07(15)
C2–C3–C4–C5	1.2(2)
C2–C3–C4–C14	−179.25(15)
C49A–C48A–C53A–C52A	−5(3)
C47A–C48A–C53A–C52A	−177(2)
C60–C55–C56–C57	1(3)
C54–C55–C56–C57	177.2(15)
C55–C56–C57–C58	−1(3)
C56–C57–C58–C59	1(2)
C57–C58–C59–C60	−1(2)
C58–C59–C60–C55	2(2)
C56–C55–C60–C59	−1(2)
C54–C55–C60–C59	−177.7(14)
C60A–C55A–C56A–C57A	3(3)
C54A–C55A–C56A–C57A	−177(2)
C55A–C56A–C57A–C58A	0(3)
C56A–C57A–C58A–C59A	−3(3)
C57A–C58A–C59A–C60A	4(3)
C58A–C59A–C60A–C55A	−1(3)
C56A–C55A–C60A–C59A	−3(3)
C54A–C55A–C60A–C59A	177.7(19)

Bonds to hydrogen atoms were omitted.

Table S10. Comparison of Ta–N bond lengths and bond lengths within the NNN pincer ligand for Ta complexes with different ligand oxidations states.

Bond length	Ligand in catecholate form		Ligand in semiquinone form		Ligand in quinone form
	I	**4**	**II**	**5**	**3**
Ta1–N1	2.001(3)	2.0080(19)	2.042(2)	2.028(3)	2.158(3)
Ta1–N2	2.037(2)	2.0316(19)	2.161(2)	2.136(4)	2.218(2)
Ta1–N3	1.992(3)	2.0138(19)	2.043(2)	2.025(3)	2.153(2)
N1–C2	1.403(5)	1.400(3)	1.371(5)	1.380(4)	1.346(3)
C2–C1	1.399(4)	1.400(3)	1.408(6)	1.418(3)	1.451(4)
C1–N2	1.389(4)	1.394(3)	1.361(5)	1.356(4)	1.323(4)
N2–C13	1.391(4)	1.390(3)	1.362(5)	1.352(3)	1.388(4)
C13–C12	1.399(4)	1.406(3)	1.422(6)	1.420(4)	1.439(4)
C12–N3	1.401(4)	1.390(3)	1.373(6)	1.366(3)	1.353(3)

Computational Details

Table S11. Calculated free Gibbs energies of complexes, the hydrogen atom and the free energies for comproportionation of **1** and **3** to give **2**.

Compound	**Free Gibbs energy in kcal/mol**	
	Gas phase	**benzene**
1	-1457251.043	-1457257.926
2	-1456861.983	-1456868.798
2_eq	-1456861.155	-1456867.561
3	-1456480.017	-1456488.033
Hydrogen atom	-319.196	-319.251
Comproportionation of **1** and **3**	7.09	8.36

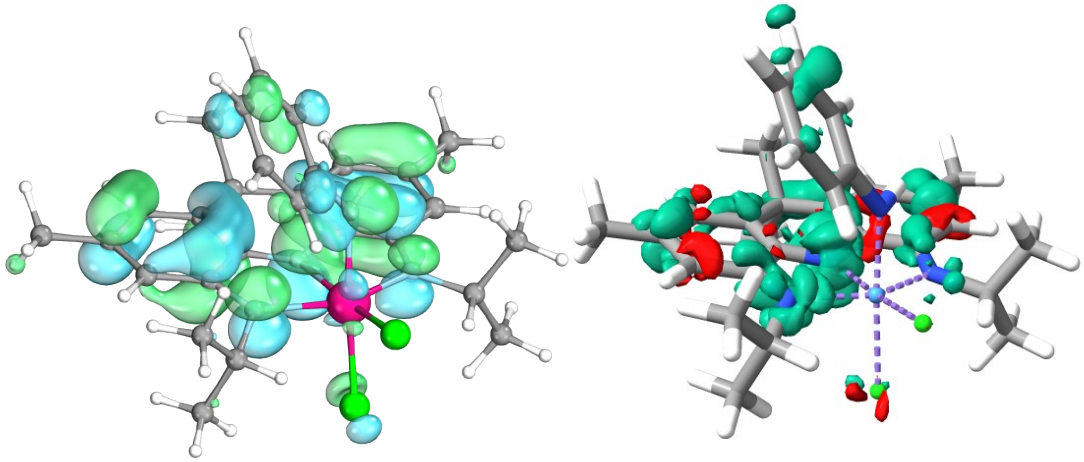

Figure S36. Calculated SOMO and spin density of **2**.

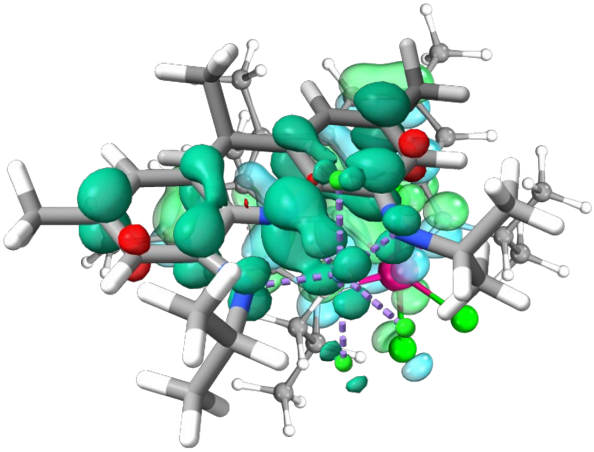

Figure S37. Calculated SOMO and spin density of **4**.

To determine the bond dissociation free energies of the N–H bonds of **1** and **2** the following reaction energies were calculated in the gas phase and in benzene

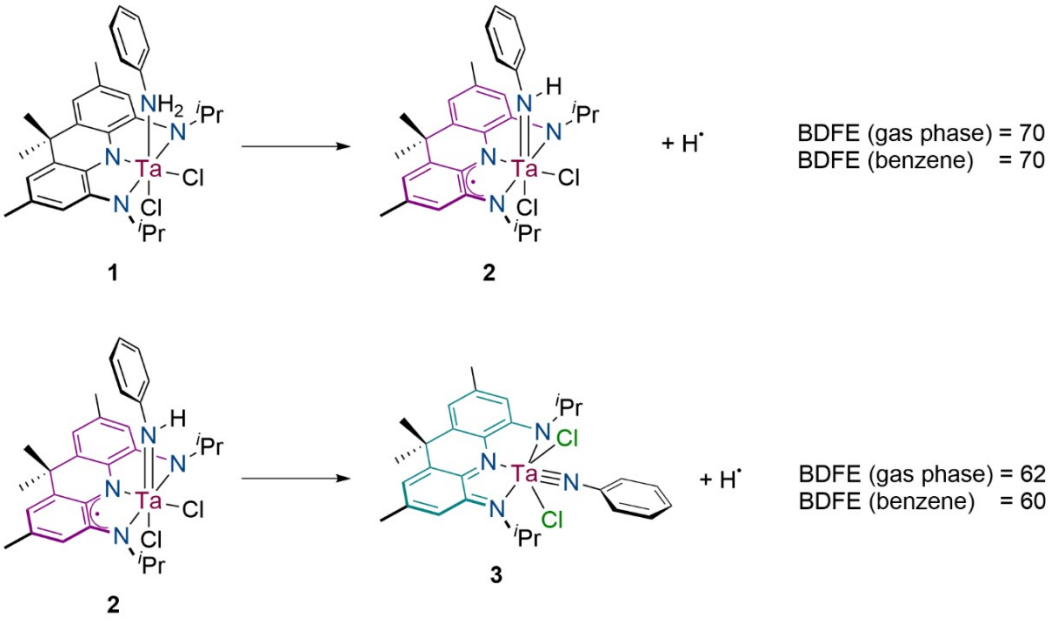

Figure S38. Calculated bond dissociation free energies of **1** and **2**.

References

[1] F. You, J. Zhai, Y.-M. So and X. Shi, *Inorg. Chem.*, 2021, **60**, 1797–1805.
[2] E. W. Y. Wong and D. J. H. Emslie, *Dalton Trans.*, 2015, **44**, 11601–11612.
[3] J. Underhill, E. S. Yang, T. Schmidt-Räntsch, W. K. Myers, J. M. Goicoechea and J. Abbenseth, *Chem. Eur. J.*, 2023, **29**, e202203266.
[4] A. J. King, J. Abbenseth and J. Goicoechea, *Chem. Eur. J.*, 2023, **29**, e202300818.
[5] H. Liu, N.-D. Wang and D.-M. Du, *Lett. Org. Chem.*, 2010, **7**, 114–120.